Graphical Abstract

A Techno-economic Analysis of Distributed Energy Resources versus Wholesale Electricity Purchases for Fueling Decarbonized Heavy Duty Vehicles

An T. Pham, Larson Lovdal, Tianyi Zhang, Michael T. Craig

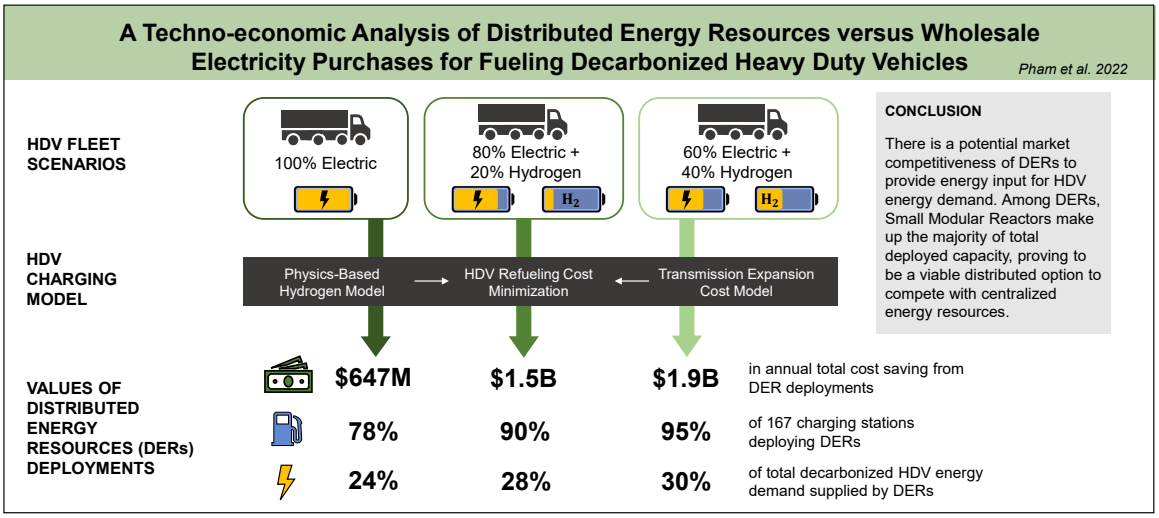

Highlights

A Techno-economic Analysis of Distributed Energy Resources versus Wholesale Electricity Purchases for Fueling Decarbonized Heavy Duty Vehicles

An T. Pham, Larson Lovdal, Tianyi Zhang, Michael T. Craig

- We create a model to quantify the value of distributed energy resources for meeting decarbonized heavy duty vehicle energy demand.
- Distributed energy resources are deployed at 78% to 95% of all charging stations.
- Annual cost savings from distributed energy resources investments can be as high as $1.9 billion nation-wide, and $104 million at an individual station.
- Small modular microreactors supply approximately between 24% and 30% of heavy duty vehicle energy demand annually.

A Techno-economic Analysis of Distributed Energy Resources versus Wholesale Electricity Purchases for Fueling Decarbonized Heavy Duty Vehicles

An T. Pham[a], Larson Lovdal[a,b], Tianyi Zhang[a,b], Michael T. Craig[a]

[a]*School for Environment and Sustainability, University of Michigan, 440 Church St., Ann Arbor, MI 48109, USA*

[b]*Mechanical Engineering, University of Michigan, 2350 Hayward St., Ann Arbor, MI 48109, USA*

Abstract

Electric and hydrogen vehicles can help decarbonize heavy duty vehicles (HDV). Few studies examine how to meet energy requirements of decarbonized HDVs, and all assume electricity will come from centralized systems. However, decarbonized HDVs could significantly increase energy demands in areas with limited transmission access, potentially favoring deployment of distributed energy resources (DERs). In this paper, we develop an optimization-based techno-economic model that minimizes costs of meeting HDV energy demands by optimizing investments in and operations of DERs, investments in transmission interconnections, and wholesale electricity purchases. We apply it to a modeled U.S. dataset of electric HDV charging demands to quantify the deployment and value potential of three DERs - solar, batteries, and nuclear small modular reactors (SMRs) in the year 2040. For fleets of 100% electric HDVs to 60% electric and 40% hydrogen HDVs, DERs are deployed at 78% to 95% of all charging stations and meet between 24% to 30% of total HDV energy demand. Investments in DERs reduce annual costs by $647 million to $1.9 billion across all stations, while individual stations can save $20 million to over $100 million annually. SMRs make up over 99% of total deployed DER capacity, indicating significant potential for SMR deployment in this emerging market. Widespread DER deployment is robust to capital cost uncertainty in SMRs and transmission lines, wholesale electricity prices, and other factors.

Keywords: distributed energy resources, small modular reactors, decarbonized heavy duty vehicles, transportation sector decarbonization

1 Introduction

To limit global average temperature increases to 1.5°C or 2°C above pre-industrial levels, greenhouse gas (GHG) emissions in developed countries must rapidly decline through 2050 [1]. In the United States, the transportation sector surpassed the electricity sector as the largest source of GHG emissions in 2017 [2]. In 2019, the transportation sector was responsible for 29% of national GHG emissions, with further emissions growth expected [3, 1]. To reduce the sector's emissions in line with climate change mitigation goals, transitioning from liquid petroleum fuels to alternative fuels is critical. Heavy duty vehicles (HDVs), defined as class 7 and class 8 trucks, which are vehicles with gross vehicle weight rating above 26,001 lbs [4], were the fastest growing source of global oil demand for the last two decades [5], accounting for roughly 40% of GHG emissions from the global transportation sector [6]. Without any further policy efforts, global oil demand is expected to continue to grow at least through 2035 at an average annual growth rate between 1.13% and 5% [7, 5], mostly due to increase in global road freight demand [5, 8]. Thus, decarbonizing the HDV fleet is essential to decarbonize the transportation sector. This transition is just beginning for HDVs, as they pose a larger decarbonization challenge than light or medium duty vehicles (LDVs or MDVs). While electrification of LDVs and MDVs has rapidly progressed [9], electrifying HDVs is challenged by heavier battery weights and higher power requirements for fast charging [10, 11]. Hydrogen is an alternative promising decarbonization pathway for HDVs, but remains in early stages of development and deployment [12, 13, 14, 15, 16, 17].

Many electrified end uses, including electrified light-duty vehicles, will increase demand in densely populated areas with ample transmission system access [18]. Conversely, given their long-distance hauls, decarbonized HDVs could introduce significant new energy demands in sparsely populated areas with limited transmission system access

[19]. Meeting these new demands through the centralized power system could require significant transmission investments, which could be challenged by costs and social resistance [20, 21]. Distributed energy applications could avoid these complications [22] while serving the emerging potential market of providing energy input for decarbonized HDV charging demand. The estimated increase in electricity demand due to decarbonization of the HDV fleet will be significant [19]. Charging a single electric HDV could increase electricity demand by as high as 2.5 MW in an hour, and total HDV energy demand for one NERC region could be as high as 175 GWh daily [19].

Few studies have examined how to meet energy requirements for decarbonized HDVs. [16] couple a centralized infrastructure planning model with a power system optimization model in Germany to study the power system implications of different designs of fuel cell HDV refueling networks. They find cost savings when planning for fuel cell HDV and power system infrastructure together rather than independently. [19] meet charging demand at each of 219 charging stations assuming 100% of the HDV fleet is electrified across the U.S. They meet this demand by dispatching existing generators in the bulk (or centralized) power system, then quantify emissions changes due to HDV charging demand.

These papers offer valuable insights into the physical and technical feasibility of decarbonizing HDVs. However, they both assume that decarbonized HDV demand is met fully by centralized electricity generation, and either ignore [19] or significantly simplify [16] the cost of transmission expansion for connecting HDV charging stations with the centralized grid. We extend this existing literature in two novel ways. First, we quantitatively evaluate distributed energy options for meeting energy demands of decarbonized HDVs, and compare distributed to centralized energy options. Second, in considering centralized energy options, we account for spatially- and capacity-differentiated transmission expansion costs. Spatially-differentiated costs reflect locations of transmis-

sion lines and charging stations, while capacity-differentiated costs reflect the capacity of power purchased by charging stations from the bulk power system.

Using this new novel framework, this paper studies the feasibility of distributed energy resources (DERs) for meeting energy demands of decarbonized HDVs, as opposed to centralized energy resources. All DERs need to compete among each other and with centralized energy resources on economic and technical grounds to provide electricity and/or hydrogen to decarbonize the HDV fleet. Distributed systems could include existing technologies, such as solar photovoltaics (PV) or batteries, or emerging technologies. Two such emerging technologies that have promising potential are nuclear small modular reactors and microreactors (which we will collectively refer to as SMRs). Microreactors have nameplate capacities between 1 and 20 MW [23], while small modular reactors can be sized up to 300 MW [24]. The small size of SMRs grants them greater siting flexibility than conventional nuclear plants [25], and their construction can occur via mass fabrication, potentially enabling large cost reductions through economies of number and component-based learning [25, 26, 27]. Due to these advantages, studies are beginning to consider SMRs in niche electricity and/or industrial thermal markets [22, 28, 29, 30], including in remote settings [31, 32]. [24] also assess the value of SMRs in niche and large electricity and thermal markets using a simplified levelized cost of energy approach that ignores SMR operational needs to meet a given end use demand. These studies share two significant gaps. First, they do not optimize deployment and operations of SMRs in an emerging market given competition from centralized and decentralized energy resources. Second, they do not consider SMR deployment to meet decarbonized HDV energy demands, despite the potential benefits of this match as detailed above.

We fill critical gaps in two areas of literature: (1) understanding how to meet emerging energy demands of decarbonized HDVs and (2) understanding viable markets for SMR deployment (Table 1). To fill these gaps, we answer the following research questions:

How can decarbonized HDV energy demand be met with distributed versus centralized energy, and what role, if any, can SMRs play in this emerging market? To answer these research questions, we develop an optimization-based techno-economic model to compare the value of different DERs (including SMRs) versus centralized energy resources for charging electric and/or refueling hydrogen HDVs (collectively referred to as HDV energy demand) in the year 2040. Given the uncertainties in the availability and scalability of future technologies and policy constraints, as well as future wholesale electricity prices, we also perform sensitivity analyses to test the robustness of our results under a wide range of capital costs, infrastructure upgrades, infrastructure utilization, and different modeled years corresponding to different wholesale electricity price scenarios.

While prior work has used macro-scale power system models to understand how HDV demands change bulk power system operations, our novel framework instead quantifies the value of distributed energy resources versus centralized power purchases for meeting HDV demands.

Paper	Methods	Study focus	Gaps
Literature on meeting decarbonized HDV demand:			
[16]	Power system model	Power system implications of different hydrogen HDV refueling network designs	No DER consideration; simple assumptions about the cost of connecting refueling stations to the power grid
[19]	Truck dispatch and economic dispatch	Meet charging demand assuming 100% electrified HDV fleet	No DER consideration; no transmission expansion cost
Literature on SMR applications:			
[22], [28] [29], [30]	Summary ; economic comparisons; estimation	Discussion of SMR applications in small niche markets	No application in HDV market; no SMR operation and deployment optimization
[31], [32]	Cost analysis	Discussion of SMR applications in remote settings	No application in HDV market; no SMR operation and deployment optimization
[24]	Simplified levelized cost of energy	Estimates of SMR costs in large thermal/energy markets	No SMR operation and deployment optimization

Table 1: Review of current strands of literature

2 Methods

To answer our research questions, we use an optimization-based techno-economic model to compare the value of distributed versus centralized energy resources for charging electric and/or hydrogen HDVs (hereafter referred to as the HDV Charging Model) (Figure 1). The HDV Charging Model optimizes investments in DERs, operations of those investments, investments in transmission lines to access the bulk power system, and wholesale electricity purchases enabled by those transmission investments. The model runs on an hourly basis for a calendar year using annualized capital costs and combines highly spatially resolved datasets for future station locations, transmission system access, and solar resources. With model outputs, we quantify investments, operations, and

fixed and variable costs to meet energy demand from decarbonized HDVs. By modifying investment options in the model via scenarios, we quantify the value of different technologies in charging and/or refueling decarbonized HDVs.

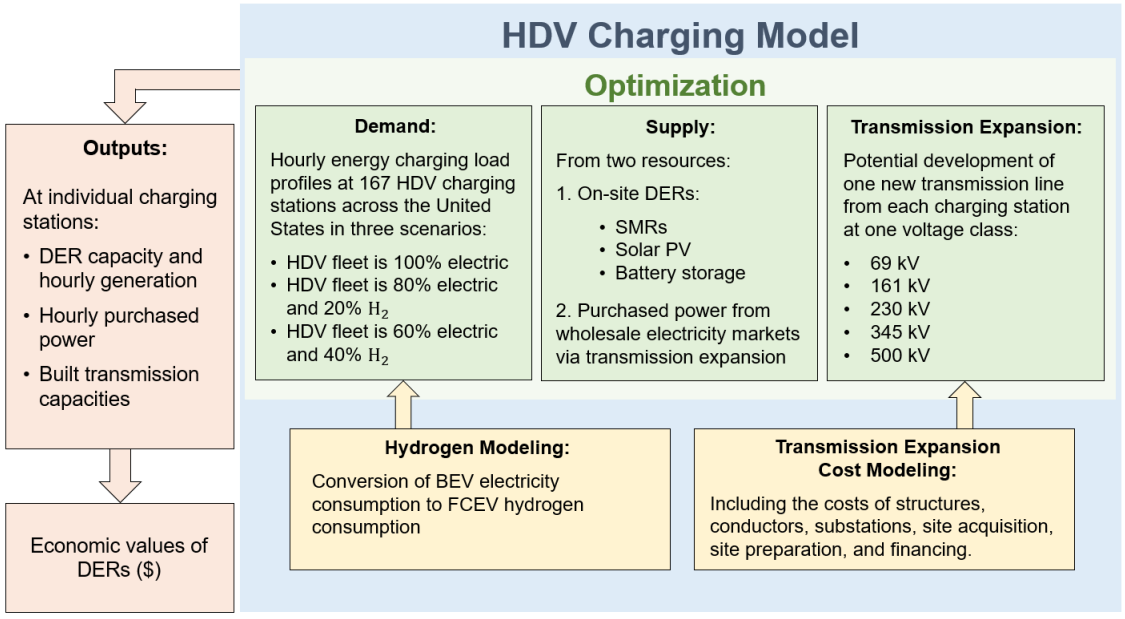

Figure 1: Flowchart of HDV Charging Model.

2.1 Overview of HDV Charging Model

The HDV Charging Model minimizes total annual costs of meeting HDV energy demand at the charging station level. Annual total costs equal the sum of capital costs in transmission and DERs; operational costs of transmission infrastructure and distributed energy capacity resources; and wholesale electricity purchase costs as detailed in equation (1).

$$
\begin{aligned}
TC_s = \quad & \left[p^{BK} k_s^B + p^{BC} e_s^B + \sum_t p^{BE} g_{st}^B \right] + \left[p^{HK} k_s^H + p^{HC} e_s^H + \sum_t p^{HE} g_{st}^H \right] \\
& + \left[p^{PK} k_s^P + \sum_t p^{PE} g_{st}^P \right] + \left[p^{MK} u_s^M \bar{k}^M + \sum_t p^{ME} g_{st}^M \right] \\
& + \left[\sum_i \left(1 + p^{WO}\right) p_{si}^{WK} \bar{k}_{si}^W u_{si}^W + \sum_t p_{st}^{WE} g_{st}^W \right] \qquad (1)
\end{aligned}
$$

where p^{BK} is the annualized battery power rating cost (\$/MW-year), k_s^B is the battery power rating at charging station s (MW), p^{BC} is the battery energy capacity cost (\$/MWh), e_s^B is the battery energy capacity at station s (MWh), p^{BE} is the battery operating cost (\$/MWh), g_{st}^B is battery discharge in time t at charging station s (MWh), p^{HK} is the annualized hydrogen power rating cost (\$/MW-year), k_s^H is the hydrogen power rating at charging charging station s (MW), p^{HC} is the hydrogen energy capacity cost (\$/kg), e_s^H is the hydrogen energy capacity at station s (kg), p^{HE} is the hydrogen operating cost (\$/kg), g_{st}^H is the hydrogen discharge in time t at charging station s (kg), p^{PK} is the annualized solar capital cost (\$/MW-year), k_s^P is the solar capacity at charging charging station s (MW), p^{PE} is the solar operating cost (\$/MWh), g_{st}^P is solar generation in time t at charging station s (MWh), p^{MK} is the annualized SMR capital cost (\$/MW-year), $\bar{k}^M$ is the SMR module capacity (MW), u_s^M is the (whole) number of SMR modules built at charging station s, p^{ME} is the SMR operating cost (\$/MWh), g_{st}^M is the SMR generation in time t at charging station s (MWh), p_{si}^{WK} is the annualized total transmission capital and operating cost for station s of capacity class i (\$/MW-year), $\bar{k}_{si}$ is the effective capacity of transmission line at station s of class i (MW), u_{si}^W is the binary number indicating whether or not a transmission line of capacity class i at charging station s is built, p_{st}^{WE} is the wholesale electricity price at charging station s at time t (\$/MWh), g_{st}^W is the elec-

tricity generation purchased from the wholesale electricity markets in time t at charging station s (MWh), and p^{WO} is overhead cost in percentage.

The model enforces several demand- and supply-side constraints. The model ensures hourly energy supply meets charging demand at each charging station for both electricity, detailed in equation (2a), and hydrogen, detailed in equation (2b).

$$g_{st}^{B} + g_{st}^{P} + g_{st}^{M} + g_{st}^{W} \geq d_{st}^{E} + d_{st}^{B} + \left(\frac{1}{c^{H}}\right) d_{st}^{H}, \; \forall s \in \mathbb{S}, \; \forall t \in \mathbb{T}, \tag{2a}$$

$$g_{st}^{H} \geq \bar{d}_{st}^{H}, \; \forall s \in \mathbb{S}, \; \forall t \in \mathbb{T} \tag{2b}$$

where d_{st}^{E} is total electricity demand in time t at charging station s (MWh), d_{st}^{B} is the battery inflow in time t at charging station s (MWh), d_{st}^{H} is hydrogen inflow in time t at charging station s (kg), c^{H} is the conversion factor between battery electricity and hydrogen, and $\bar{d}_{st}^{H}$ is the total hydrogen demand in time t at charging station s (kg).

Electricity generation by each SMR is constrained by minimum stable load and ramping constraints:

$$g_{st}^{M} \geq g_{min}^{M}, \; \forall s \in \mathbb{S}, \; \forall t \in \mathbb{T}, \tag{3a}$$

$$\|g_{st}^{M} - g_{s(t-1)}^{M}\| \leq r_{s}^{M} u_{s}^{M} \bar{k}^{M}, \; \forall s \in \mathbb{S}, \; \forall t \in \mathbb{T} \tag{3b}$$

where g_{min}^{M} is the minimum stable load of SMR in a given hour, r_{s}^{M} is the ramping constraint for SMR at charging station s, measured in percentage of the resources' nameplate capacities. For storage technologies (battery and hydrogen storage), the model enforces state of charge constraints:

$$x^B_{st} = x^B_{s(t-1)} + d^B_{st} - g^B_{st},\ \forall s \in \mathbb{S},\ \forall t \in \mathbb{T}, \tag{4a}$$

$$0 \leq x^B_{st} \leq e^B_s,\ \forall s \in \mathbb{S},\ \forall t \in \mathbb{T}, \tag{4b}$$

$$x^H_{st} = x^H_{s(t-1)} + d^H_{st} - g^H_{st},\ \forall s \in \mathbb{S},\ \forall t \in \mathbb{T} \tag{4c}$$

$$0 \leq x^H_{st} \leq e^H_s,\ \forall s \in \mathbb{S},\ \forall t \in \mathbb{T}, \tag{4d}$$

where x^B_{st} (x^H_{st}) is the state of charge of battery (hydrogen) storage at station s at time t, and $x^B_{s(t-1)}$ ($x^H_{s(t-1)}$) is the battery (hydrogen) storage's state of charge at the same station in the previous hour. Hydrogen storage takes electricity input, either from on-site distributed resources (solar PV, battery storage) or from purchased electricity from the grid, and is used to refuel hydrogen HDVs only. The model does not consider the case where hydrogen storage can produce electricity to supply electric HDVs. For solar PV, the model limits hourly generation by on-site solar PV at each charging station based on available hourly solar resources.

$$0 \leq g^B_{st} \leq f^P_{st} k^P_{st},\ \forall s \in \mathbb{S},\ \forall t \in \mathbb{T}, \tag{5}$$

where f^P_{st} is solar PV capacity factor in percentage at station s at time t.

The model is programmed in Pyomo (Python) and solved using CPLEX Version 20.1.0.1.

Our model's high spatiotemporal resolution allows us to capture crucial trade-offs between distributed and centralized energy solutions that will drive the value of future DER deployment at HDV charging stations. Alternative analytical approaches, e.g. macroscale energy system models, would better capture regional interactions across HDV charging stations. However, these alternative approaches are computationally intensive, so require significant spatiotemporal simplifications that could lessen their value at capturing

DER versus centralized energy solutions for HDV charging stations. We suggest alternative approaches be used in future work, guided by the insights generated through our analytical approach.

2.2 Transmission Expansion Cost Modeling

To capture the cost of purchasing electricity from wholesale markets, our model includes two relevant categories: transmission expansion costs and wholesale electricity purchase costs. We assume each station requires additional transmission capacity to serve new electrical load and estimate the cost of constructing a new transmission line for both single and double circuit lines at 5 voltage classes (69kV, 161kV, 230kV, 345kV, and 500kV). Costs are developed primarily using the methodology and data in [33] with a modified land cost method to generalize the framework beyond the Midcontinent Independent System Operator (MISO) territory as illustrated in Figure 2 and described below.

For a given station, we measure the straight line distance from the station to the nearest existing transmission line of each capacity class using ArcGIS Pro 2.8 [34]. Existing transmission infrastructure data is drawn from the Homeland Infrastructure Foundation Level Database Electric Power Transmission Lines layer [35] and lines are binned into the five voltage classes previously described. Given that a single line cannot provide sufficient power for a double circuit of the same voltage, double circuit lines are routed to the nearest point at least one voltage class above (i.e. 69 kV double circuit connects to at least 161 kV etc.) with double circuit 500kV lines interconnecting to existing 735kV infrastructure.

To calculate total land costs, we sum acquisition, permitting, and right-of-way preparation (e.g. clearing trees, grading) costs. To find these values, we combine the area along each route with acquisition costs per acre [36], land cover types [37] and preparation costs [33], and permitting expenses [33]. At each station and capacity class land

costs are summed together with conductor and structure (tower) costs to find the transmission line capital subtotal as detailed in Appendix C.5. Following [33], a 30 percent contingency is added to the straight-line estimate recognizing that a new line likely could not be built along the absolute shortest path.

Substation costs are added assuming a new substation is built at each end of the line. We apply a 17.5% overhead and 30% contingency allowance to the subtotal to produce a total estimated capital expense, which is annualized using a capital recovery factor (CRF). Finally, annual operating and maintenance expenses for both the transmission line ($7,300.75 per circuit mile) and substation ($1,543.65 per MVA) are estimated based on an average from 17 and 12 large utilities respectively [38]. Further detail on the transmission line expansion methods and data can be found in section Appendix C.5 in the SI.

While the cost estimates include a substation at each end of a new line, they do not include any distribution infrastructure between the substation and charging station. Similarly, estimates for new distributed assets (solar, SMR/microreactors) do not include any new distribution infrastructure. These costs are omitted because it is impractical to develop reasonable estimates without detailed design beyond the scope of this study and because we hypothesize that the required infrastructure would be similar across scenarios (i.e. new local distribution requirements would be similar for a solar facility, SMR, or transmission interconnection, excluding the substation). One additional limitation of the transmission expansion model is the model does not consider interaction among charging station loads, which could lead to underestimating expansion costs because multiple stations with demand profiles whose sum exceeds existing capacity can interconnect to the same transmission line.

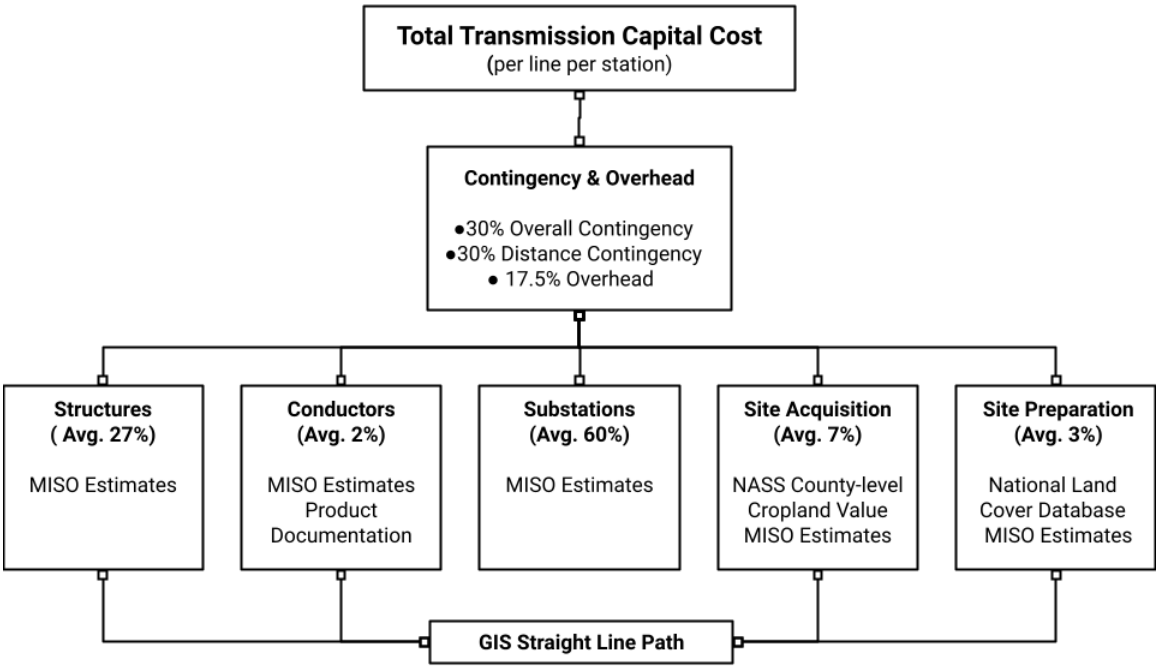

Figure 2: Transmission expansion capital cost modeling approach and data sources. Percentages are the average contribution of each subcategory to the total line capital cost across all stations and voltage classes. Bulleted items in the cost subcategories are the primary data sources.

2.3 Hydrogen Modeling

To include hydrogen HDVs in our decarbonized HDV fleet, we convert a portion of the energy consumption of electric HDVs from [19] to hydrogen demand. To do this, first, we employ a simplified physics-based model to calculate the ratio of energy consumed by hydrogen versus electric HDVs 'at the wheels' based on differing vehicle weights and power train efficiencies. We use a Monte Carlo simulation to quantify the distribution of possible energy consumption ratios given the range of vehicle parameters reported in the literature (Appendix Table A.1). The mean value of the resulting distribution is used to convert energy demand of electric HDVs (in kWh) to equivalent energy demand for hydrogen HDVs (still in kWh). Second, we convert the hydrogen HDV energy demand (in kWh) to hydrogen demand (in kg) using the higher heating value of hydrogen.

We model on-site hydrogen production via electrolysis and above-ground hydrogen storage. The electricity demand for producing H_2 is calculated by multiplying hydrogen demand by an electrolyzer conversion ratio. We use above-ground storage as underground caverns for hydrogen storage might not exist at our analyzed HDV charging stations. Further details of how we model hydrogen HDVs are in Appendix B.9.

2.4 Data

We apply the HDV Charging Model for one year for each of 167 HDV charging stations, whose locations and electricity load profiles are obtained from [19]. [19] determine daily electricity load profiles at individual charging stations that would result from 100% electrification of the current inter-state HDV fleet. [19] optimize charging station locations and daily load profiles using a truck dispatch model that takes into account truck flows, driving conditions, departure schedules, and other factors. To generate annual electricity load profiles, we assume each charging stations' daily load profile repeats for the entire year. We remove three charging stations from our study - two stations for having flat demands due to [19]'s assumptions and one station for requiring over-water transmission line development to get access to bulk power, which we do not have a good cost estimate for. We choose to base our study on the year 2040 when electric and hydrogen HDVs could be deployed at large scale, and when SMR technology could be mature enough to be a viable DER option.

Data for fixed O&M cost and capital costs for battery storage and solar PV are taken from U.S. National Renewable Energy Laboratory (NREL)'s 2020 Electricity Annual Technology Baseline [39]. To annualize capital costs, we apply a capital recovery factor using a discount rate of 3% per federal guidance [40]. This interest rate is also within a reasonable range of discount rates for SMRs [24]. Solar capacity factors at the locations of the charging stations are calculated by [41] using solar resource data from NREL's Na-

tional Solar Radiation Data Base (NSRDB) in 2014. The hourly costs of purchasing energy from the wholesale markets to serve charging stations' demands are taken from NREL's Cambium dataset [42]. To reflect the long lead time to a fully electrified HDV fleet, we use wholesale electricity prices for 2040. Wholesale prices for each station equal the projected hourly marginal energy prices at the balancing authorities in which each station is located.

We obtain capital and operational costs of SMRs from [43], which details data input for SMRs from NuScale LLC, a major developer of SMRs that has one of the most advanced SMR technologies to date. We obtain capital and operational costs of microreactor from [24], which conducts a thorough evaluation of the cost of electricity and heat from microreactors of 10 MW nameplate capacity. Details of SMR and microreactor data input can be found in Table A.5 in the SI.

For hydrogen HDVs, we impute a conversion factor of electricity demand of electrified HDVs to hydrogen demand of hydrogen HDVs of 0.0471 kg/kWh (Appendix B.9). Capital cost of hydrogen electrolyzers is obtained from [44] and the cost of storing hydrogen in above-ground hydrogen storage is obtained from [45]. Finally, the electricity to hydrogen production ratio via electrolyzer is taken from [46]. Details of hydrogen inputs can be found in Table A.3 in the SI.

Summary of capital and operational costs for the DERs studied in this paper are detailed in Table 2.

DER Technology	CAPEX $/kW	Fixed O&M Cost $/MW-year	Energy Cost $/kWh/h ($/kg/h)	Variable O&M Cost $/kWh ($/kg)	Data Source
SMR	$2,616.00	$25.00	–	$8.71	[43]
Battery Storage	$1,455.00	$36.37	$0.00	$0.00	[39]
Hydrogen Storage	$1,058.00	$0.00	$39.4	$0.00	[44, 45]
Solar PV	$1,354.00	$19.00	–	$0.00	[39]

Table 2: Capital and operational costs of different DERs for year 2040. Parenthesis indicate units for hydrogen storage. Values are in 2018$.

The effective transmission capacity at each voltage class at individual charging station level is calculated as the theoretical power capacity by voltage class, taken from [33], minus Ohmic losses along the line. Ohmic losses are calculated as the length of the transmission line times the conductor's electrical resistance per unit length times the current squared. Table 3 reports the medians and ranges of these effective transmission capacities across the transmission line voltage classes and charging stations.

Voltage Class	Median (Minimum - Maximum) Effective Transmission Capacity (MW)
<100 kV	139 (133 - 140)
<100 kV double	279 (262 - 278)
100-161 kV	459 (449 - 460)
161 kV double	917 (850 - 919)
200-287 kV	655 (622 - 657)
230 kV double	1,308 (1,193 - 1,313)
345 kV	1,969 (1,911 - 1,972)
345 kV double	3,919 (3,608 - 3,943)
500 kV	2,594 (2,544 - 2,597)
500 kV double	5,073 (4,764 - 5,192)

Table 3: Median, minimum, and maximum effective transmission capacity by voltage class across stations.

2.5 Scenarios and Sensitivity Analyses

Given uncertain penetrations of electrified versus hydrogen HDVs, we run six scenarios to quantify the economic impacts of DER investments with different levels of hydrogen HDV demands (Table 4). **Scenario 1**, which is the *Reference scenario*, allows DER investments at all charging stations but there are no hydrogen HDVs in the decarbonized HDV fleet. **Scenario 2** differs from the *Reference scenario* in that DERs are not an investment option. The difference between Scenario 2 and Scenario 1 captures the impacts of DER investments on costs and deployments of other technologies at the charging stations when there is no hydrogen HDV charging demand. Scenarios 3 through 6 facilitate similar comparisons with and without DER investment options but at increasing levels

of hydrogen HDV demand.

	100% Electric HDV Fleet	80% Electric+20% H_2 HDV Fleet	60% Electric+40% H_2 HDV Fleet
With DER Investment Options	Scenario 1 (Reference)	Scenario 3	Scenario 5
No DER Investment Options	Scenario 2	Scenario 4	Scenario 6

Table 4: Main scenarios of the study

To test the robustness of our results, we run several sensitivity analyses. Given cost uncertainty related to SMRs and transmission expansion, we run sensitivity analyses on lower and higher annualized capital costs of SMRs and transmission lines relative to our reference assumptions. Additionally, we assume existing transmission lines' capacities can be fully utilized for serving HDV demand, which might not be true. To capture this uncertainty, we rerun our analysis assuming new HDV demand can utilize only 30% or 50% of existing transmission capacity. Finally, due to uncertainty in the timeline of commercialization of electric and hydrogen HDVs, we run two sensitivities using wholesale electricity prices in 2030 and 2050. Relative to our reference 2040 prices, 2030 and 2050 LMPs are on average lower and higher, respectively. LMPs in 2030 through 2050 arise from electricity systems with increasing renewable energy (wind and solar PV) penetrations, from 37% in 2030 to 58% in 2050 [47]. Due to increasing renewables, LMPs become increasingly volatile through 2050. In 2030, the number of hours with electricity prices higher than $50/MWh observed at a single charging station is 270 hours, or 3% of all hours [48]. In 2040, [48] predict that a charging station could observe as many as 695 hours, or 8% of all hours, with electricity prices over $50/MWh, and the number of extremely high electricity prices (over $1,000/MWh) also increases compared to their 2020 projection. In total, we run 13 sensitivity analyses as described below.

Sensitivity Scenario	Description
SMR+10	SMR annualized capital cost is 10% more expensive
SMR+20	SMR annualized capital cost is 20% more expensive
SMR+30	SMR annualized capital cost is 30% more expensive
SMR+100	SMR annualized capital cost is 100% more expensive
SMR-10	SMR annualized capital cost is 10% less expensive
SMR-20	SMR annualized capital cost is 20% less expensive
SMR-30	SMR annualized capital cost is 30% less expensive
Trans+30	Transmission annualized capital cost is 30% more expensive
Trans-30	Transmission annualized capital cost is 30% less expensive
Util 50	Transmission lines can only be utilized up to 50% of capacity
Util 30	Transmission lines can only be utilized up to 30% of capacity
LMP 2030	Using 2030 LMPs
LMP 2050	Using 2050 LMPs

Table 5: Sensitivity analysis scenarios

3 Results

We first explore the deployment of distributed versus centralized energy resources for meeting decarbonized HDV energy demand. In this context, we then quantify the economic value provided by DERs versus relying only on centralized energy resources (or the bulk power system). Finally, we explore the robustness of our results across sensitivities.

3.1 Distributed versus Centralized Energy Resources for Meeting Decarbonized HDV Energy Demand

We find that DERs meet a large share of decarbonized HDV energy demand in a least-cost strategy. In aggregate across stations, we find DERs supply between 24% and 30% of HDV energy demand annually depending on the levels of hydrogen HDVs (Figure 3). In a 100% electrified HDV fleet (no hydrogen HDVs), total HDV energy demand is 268 TWh. The least-cost strategy uses DERs to meet 64 TWh, or 24% of HDV energy demand, and purchases from the centralized (or bulk) power system to meet the remaining 204

TWh, or 76% of HDV energy demand. When hydrogen HDV demand is 20% (40%) of total HDV energy demand, total HDV energy demand is 465 TWh (668 TWh), of which DERs supply 130 TWh (200 TWh), or 28% (30%), and centralized energy resources provide the remaining 72% (70%). Total electricity demand increases when decarbonized HDVs include increasing levels of hydrogen vehicles (Figure 3) because hydrogen HDVs have higher energy consumption per mile traveled than electric HDVs [49]. This means that hydrogen HDVs require more energy than electric HDVs to travel the same amount of distance.

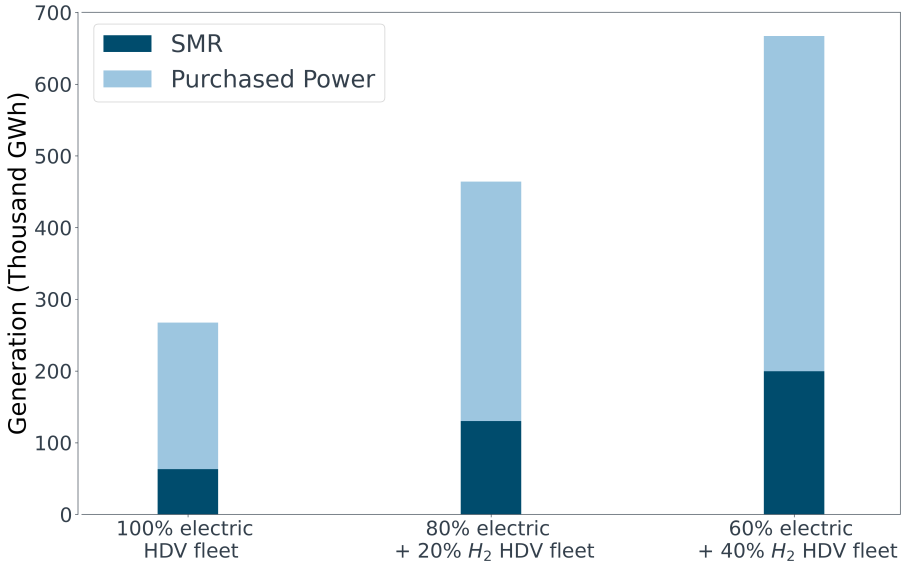

Figure 3: Total annual generation by SMRs and purchases from wholesale electricity markets. Batteries and solar generators make up of at most 1% of total generation, so are omitted from the figure.

We also find DER deployment is a widespread strategy across charging stations. Of 167 charging stations, 130 stations (or 78%) deploy distributed energy resources with a 100% electrified HDV fleet (Figure 4a). These stations in total deploy 9.79 GW of DER capacity (Table 7). The number of stations investing in DERs increases as the levels of hydrogen HDVs increases. When hydrogen HDV demand is 20% of total HDV energy

demand, 151 stations, or 90% of all stations, invest in DERs (Figure 4b), deploying in total 19.14 GW. Finally, when hydrogen HDV demand is 40% of total HDV energy demand, 159 stations, or 95% of all stations, invest in DERs (Figure 4c), deploying in total 28.23 GW.

Among DERs, the least-cost strategy deploys SMRs at significantly greater capacities than battery storage and solar PV. Under a 100% electrified HDV fleet, installed capacities of SMRs equals 9.54 GW, and installed capacity of solar PV and battery storage combined equals 0.25 GW. SMRs provide 99% of the 64 TWh of electricity generation from distributed energy resources, whereas solar PV and battery storage provide roughly 1% of electricity generation. SMRs not only provide most distributed energy generation, but also are most widely deployed across charging stations. Roughly 77% of all charging stations invest in SMRs as a DER to meet their HDV energy demand (Figure 4), and 98% of all charging stations that invest in DERs invest in SMRs. Of all charging stations that invest in SMRs, 83% invest in a 60 MW capacity SMR. The largest observed installed SMR capacity at a charging station is 240 MW without hydrogen HDVs (Figure 4a) and 1,020 MW with hydrogen HDVs (Figures 4b and 4c). Charging stations that deploy larger SMR capacities in general are located along heavily travelled truck routes, so have more constant charging demand profiles than other stations. More specifically, charging stations with higher load factors, defined as the ratio of average load over peak load, tend to deploy greater SMR capacities (Figure 5). Charging stations that do not deploy SMRs have low overall demands and load factors (between 0.13 and 0.22). The majority of charging stations that deploy more than 180 MW of SMRs have greater demands and load factors (between 0.24 and 0.51).

SMRs make up an increasing share of DER generation when there are hydrogen HDVs in the decarbonized HDV fleet. If SMRs are not available for deployment, 99.7% of total HDV energy demand is supplied by electricity bought from wholesale electricity markets.

Distributed solar and battery storage serve the remaining 0.3% of HDV demand across all charging stations. This indicates that among distributed energy resources, SMRs but not solar PV and battery storage are economically competitive with electricity purchases from the bulk power system. As hydrogen HDV demand increases to 20% (40%) of total decarbonized HDV demand, the installed capacity of SMRs equals 17.94 GW (26.28 GW), installed capacities of solar PV and battery storage combined equal 1.20 GW (1.95 GW), and SMRs account for 99.5% (99.2%) of electricity generation from DERs. SMR installed capacities increase at higher hydrogen HDV levels due to increasing SMR capacity factors. Increasing penetrations of hydrogen HDVs increase electricity demand, so SMRs generate more electricity during off-peak hours, raising SMR capacity factors. The average SMR capacity factor across all charging stations increases from 76% to 83% to 87% when increasing the share of hydrogen HDV energy demand from 0% to 20% to 40% of total decarbonized HDV energy demand.

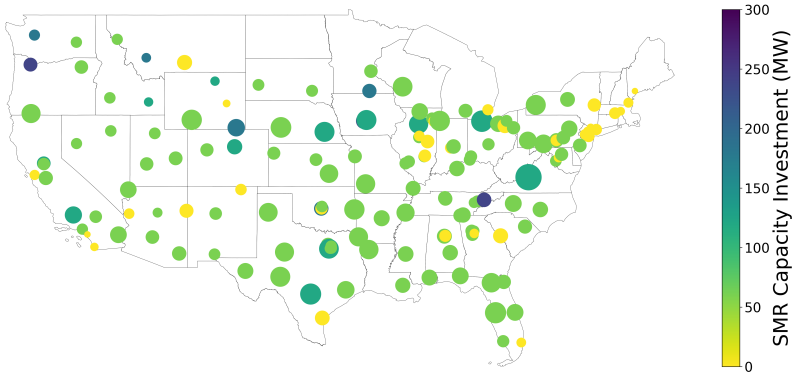

(a) 100% electric HDV fleet

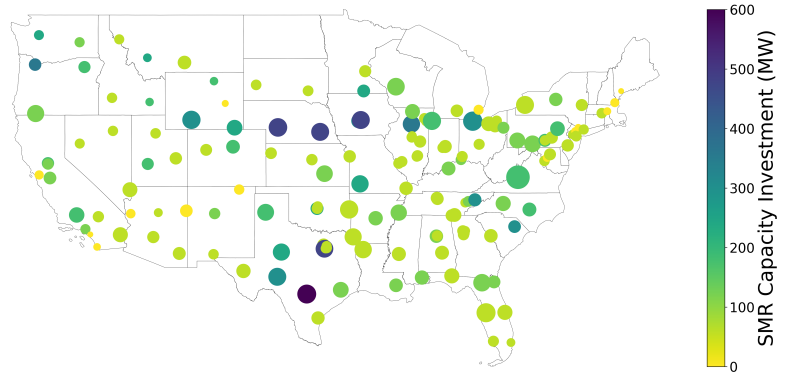

(b) 80% electric + 20% H_2 HDV fleet

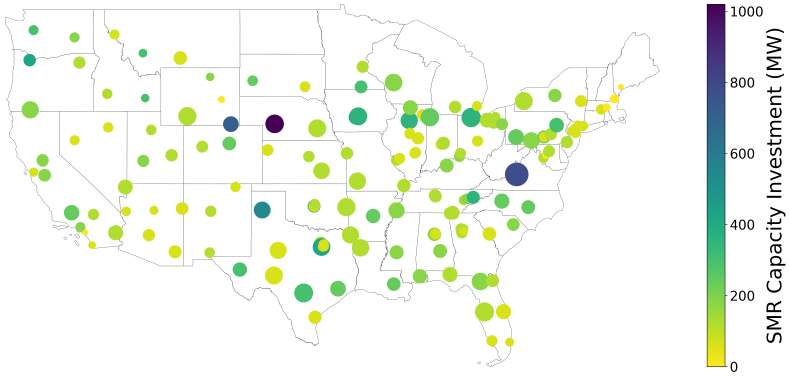

(c) 60% electric + 40% H_2 HDV fleet

Figure 4: Map of SMR deployments across 167 charging stations, at three different levels of hydrogen HDVs. The circle sizes indicate annual loads across charging stations.

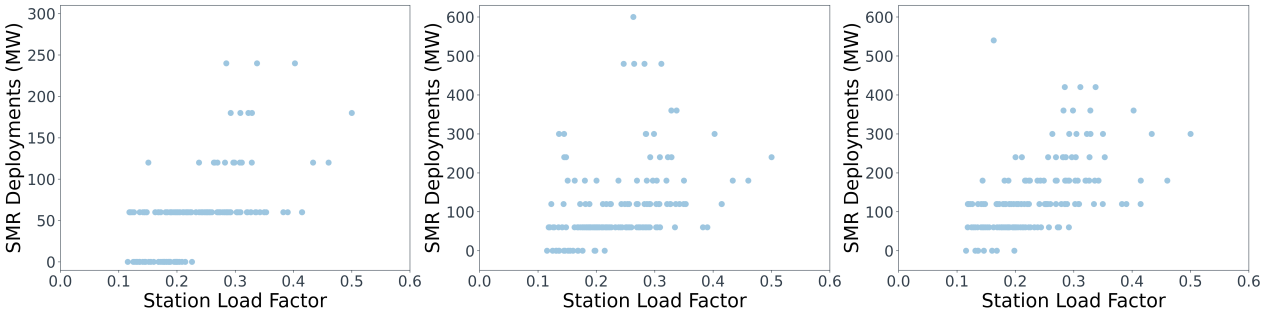

(a) 100% electric HDV fleet (b) 80% electric + 20% H_2 HDV fleet (c) 60% electric + 40% H_2 HDV fleet

Figure 5: Station load factors versus their SMR deployments.

DERs only meet a portion of load at each charging station in the least-cost solution, so all stations invest in new transmission to access power from the centralized grid. By meeting a portion of load, distributed energy deployment shifts transmission investments to lower voltage levels, regardless of hydrogen HDV levels (Table 6). Without DERs, in a 100% electric HDV fleet, 96 stations (57% of all stations) build transmission lines of voltage classes at or lower than 161 kV to purchase bulk power, while 71 stations (43% of all stations) build transmission lines above 161 kV, of which 11 stations (7% of all stations) build transmission lines of 345 kV and above. When stations invest in DERs, 109 stations (65% of all stations) build transmission lines at or lower than 161 kV, while 58 stations (35% of all stations) build transmission lines above 161 kV, of which only 5 stations (5% of all stations) need to build transmission lines of 345 kV or higher.

The impacts of DERs on transmission expansion depends on how big of a role hydrogen plays in the decarbonized HDV fleet (Figure 6). Higher levels of hydrogen HDVs increase electricity demand for decarbonized HDVs, requiring more high voltage transmission lines to be built. Some of these additional high voltage line investments can be avoided with DER deployments. When hydrogen HDV demand is 20% of total HDV energy demand, developments of 14 transmission lines of voltage classes between 230 kV

double and 500 kV are avoided due to distributed energy deployments. When hydrogen HDV demand is 40% of total HDV energy demand, expansions of 8 transmission lines of very high voltage (500 kV) and expansions of 14 transmission lines of voltage classes above 345 kV are avoided due to distribute energy deployments.

Voltage Class	100% Electric HDV Fleet	80% Electric+20% H_2 HDV Fleet	60% Electric+40% H_2 HDV Fleet
<100 kV	6 (+3)	0 (+1)	0 (0)
<100 kV double	11 (+2)	2 (-1)	1 (0)
100-161 kV	52 (+14)	7 (+5)	3 (+1)
161 kV double	27 (-6)	45 (+3)	13 (+6)
200-287 kV	43 (-1)	15 (+6)	5 (+5)
230 kV double	17 (-6)	40 (-5)	43 (+1)
345 kV	10 (-6)	38 (-1)	52 (+1)
345 kV double	0 (0)	3 (-2)	27 (-6)
500 kV	1 (0)	16 (-6)	21 (-7)
500 kV double	0 (0)	1 (0)	2 (-1)

Table 6: Number of transmission lines built in different voltage classes with DER deployments and changes in the number of transmission lines of each voltage class due to DER deployments. Numbers in parenthesis denote the change in the number of transmission lines built due to DER investments.

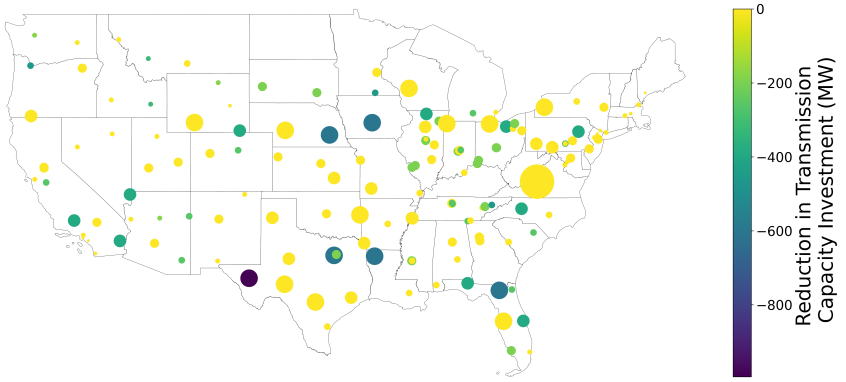

(a) 100% electric HDV fleet

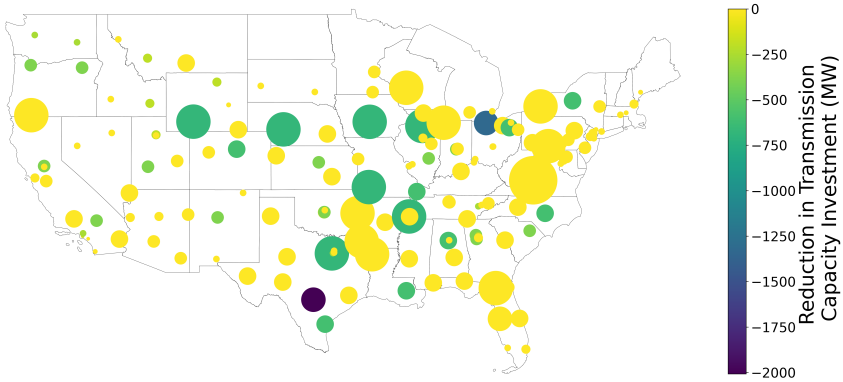

(b) 80% electric + 20% H_2 HDV fleet

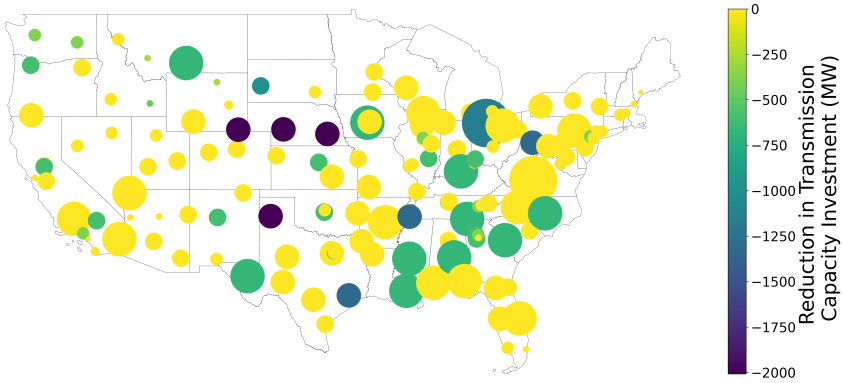

(c) 60% electric + 40% H_2 HDV fleet

Figure 6: Map of changes in transmission line expansions when DER deployments are allowed, compared to when DER deployments are not allowed in the HDV Charging Model (Table 4), across 167 charging stations, in three scenarios of different levels of hydrogen HDVs: a) 0% - Scenario 1 compared to Scenario 2, b) 20% - Scenario 3 compared to Scenario 4, and c) 40% of decarbonized HDV fleet - Scenario 5 compared to Scenario 6. The circle sizes indicate transmission capacity investments when there are no DER deployments across charging stations.

3.2 Economic Value of Distributed Energy Resources

To quantify the economic value of DERs in meeting decarbonized HDV energy demand, we calculate per-station and total costs of meeting decarbonized HDV energy demand when DERs are and are not available for deployment. When not available, charging stations must rely 100% on purchased power from wholesale electricity markets to serve HDV energy demand. In this case, the total annual cost of meeting energy demands for a fully electrified HDV fleet is $9.27 billion, of which $8.30 billion, or 90%, equals electricity purchase costs and the remaining 10%, or $0.97 billion, equal transmission expansion costs. Total annual costs increase with increasing hydrogen HDV levels because of the high capital cost of hydrogen production and storage. When hydrogen HDV demand is 20% (40%) of total HDV energy demand, the total annual cost of meeting HDV energy demands is $61.01 billion ($113.08 billion), of which $13.80 billion ($19.30 billion), or 23% (17%), equals electricity purchase costs, $45.30 billion ($90.36 billion), or 74% (80%), and the remaining 3%, or $1.91 billion (3%, or $3.42 billion), equal transmission expansion costs.

Allowing DER deployment yields total cost savings of $647 million to $1,926 million depending on hydrogen HDV levels. With a 100% electrified HDV fleet, the total cost saving of $647 million equals avoided centralized energy costs of $2,604 million minus incurred DER costs of $1,957 million. Avoided centralized energy costs include avoided $2,516 million in power purchases and $88 million in transmission upgrades. Incurred DER costs include SMR capital ($1,318 million) and generation ($600 million) costs, and battery and solar PV total cost ($39 million). Total cost savings from DERs increase with increasing hydrogen HDV demands, but the percent of total costs saved decreases because of high hydrogen-related costs. Total cost savings from DER deployment across all charging stations is $1,508 million, or 2.4%, and $1,926 million, or 1.7%, respectively,

when hydrogen HDV demand is 20% and 40% of total HDV energy demand. In these cases, total cost savings from DER investments include the avoided bulk power-related costs of $5,410 million and $10,083 million, and the incurred DER costs of $3,902 million and $8,159 million, when hydrogen HDV demand is 20% and 40% of total HDV energy demand, respectively.

	100% Electric HDV Fleet	80% Electric+20% H_2 HDV Fleet	60% Electric+40% H_2 HDV Fleet
Total Cost (Billion $)	8.62	59.51	111.15
Cost Saving (Million $)	647 (7.0%)	1,508 (2.4%)	1,926 (1.7%)
From Power Purchase	2,516	4,670	6,689
From Infrastructure Upgrades	88	740	3,394
From SMR Generation	-600	-1,233	-4,424
From SMR Deployment	-1,318	-2,479	-3,424
From Battery and Solar Costs	-39	-190	-309
DER Deployment (GW)	9.79	19.14	28.23
No. DER Investing Stations	130 (78%)	151 (90%)	159 (95%)

Table 7: Economic impacts of DER deployments.

Individual stations' cost savings from DERs, which are largely SMRs here, vary across locations and demand profiles (Figure 7). With a 100% electrified HDV fleet (Figure 7a), individual stations can save as much as $20.1 million annually, or 18.5% of their total costs, with DER deployments. When hydrogen HDV demand is 20% (40%) of total HDV energy demand (Figures 7b and 7c), individual stations can save up to $73.5 million, or 8.1% of their total annual costs ($104.9 million, or 9.0% of their total annual costs) by investing in DERs.

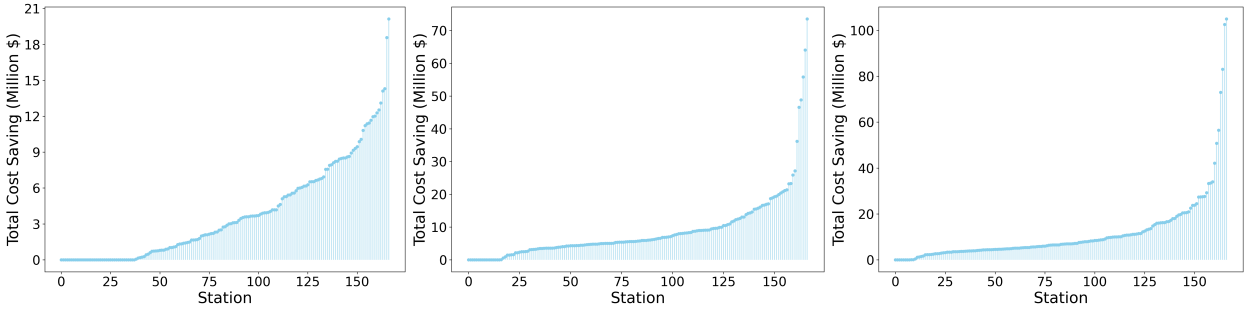

(a) 100% electric HDV fleet (b) 80% electric + 20% H_2 HDV fleet (c) 60% electric + 40% H_2 HDV fleet

Figure 7: Individual stations' cost savings from DER investments sorted from lowest to highest (million $).

3.3 Sensitivity Analyses

We perform 13 sensitivity analyses to capture uncertainty in SMR capital costs, transmission costs and utilization, and electricity prices. Table 8 reports a selection of sensitivity analysis scenarios that represent our main findings. The rest of the sensitivity analyses are in Table A.12, Table A.13, and Table A.14 in the SI.

At an annualized SMR capital cost 30% greater than reference, total DER deployment decreases by 3.76 GW, or 38%, compared to reference. This 3.76 GW difference is the net of 3.84 GW decrease in SMR deployment and 0.08 GW increase in solar PV and battery deployments. The number of stations deploying DERs also decreases by 35 stations, or 30%, compared to reference. Due to less deployment, total cost savings from DER deployment are $430 million, or 32% less than total cost savings from DER deployment in the reference case. At an extremely high annualized SMR capital cost (100% greater than reference), total DER deployment decreases to 430 MW, all of which comes from battery and solar PV at 27 charging stations. Conversely, at an annualized SMR capital cost of 30% lower than reference, total DER deployment increases by 2.86 GW, or 29%, compared to reference, of which SMR deployment increases by 3.06 GW while solar PV and battery deployments combined decreases by 0.2 GW. The number of stations deploying

DERs increases by 19 stations, or 15%, compared to reference. Total cost savings from DER deployment are $1.1 billion, which is 70% more than total cost savings from DER deployment in reference. These results indicate a sizeable market for SMRs as DERs for meeting HDV energy demand across a wide range of potential SMR capital costs.

Using 2030 electricity prices, which have the lowest annual average prices, results in a decrease in DER deployment of 1.81 GW, or 18%, compared to reference. This 1.81 GW decrease is the net of a 1.56 GW decrease in SMR deployment and a 0.25 GW decrease in solar PV and battery deployments. The number of stations investing in DERs in this case also decreases by 18 stations, or 14%, compared to reference. Using the 2050 LMP time series, which is the most volatile and higher on average than 2030 (though lower than 2040), DER deployment decreases by 770 MW, or 8%, compared to reference. This 770 MW decrease is the net of a 720 MW decrease in SMR deployment and a 50 MW decrease in solar PV and battery deployments. The number of stations investing in DER in this case decreases by 3 stations, or 2%, compared to reference. These results indicate that the higher and more volatile LMPs, the higher DER deployments and more stations investing in DERs. The market for DERs proves to be viable in all of the LMP time series we run in this analysis; at least 67% of all stations invest in DERs in the least-cost solution regardless of LMPs.

An increase or decrease of 10%, 20%, or 30% in transmission capital cost has little impact on total capacity of DERs deployed or the number of stations investing in DERs (Table 8 and Table A.13). Similarly, limiting transmission line utilization to 50% or 30% of the technical capacity has minimal effects on DER deployments and stations' decisions to invest in DERs.

	Reference	SMR +30	SMR +100	SMR -30	Util 30	LMP 2030	LMP 2050
Total Cost (Billion $)	8.62	8.94	9.24	8.17	9.19	8.55	8.59
Saving (Million $)	647	430	30	1,103			
	(7.0%)	(4.6%)	(0.3%)	(11.9%)			
DER Deployment (GW)	9.79	6.03	0.43	12.65	13.63	8.09	9.02
SMR Deployment (GW)	9.54	5.70	0.0	12.60	11.70	7.98	8.82
No. DER Investing Stations	130	95	27	149	128	112	127
	(78%)	(57%)	(2%)	(89%)	(76%)	(67%)	(76%)

Table 8: Selected Sensitivity Analyses

4 Discussion

This paper examined the cost effectiveness of distributed energy resources versus centralized energy resources to provide energy for a decarbonized HDV fleet in the U.S. We considered two types of DERs: mature technologies that are already widespread (solar PV and battery storage) and emerging technologies (SMRs). We quantified the aggregate and individual charging station-level cost savings from investing in on-site DERs to supply HDV energy demand when the HDV fleet is all electric and when the HDV fleet is part electric, part hydrogen. To do this, we used an optimization-based techno-economic model to compare the values of DERs against centralized energy resources for providing electricity and/or hydrogen input for the decarbonized HDV fleet across the U.S. Our model accounted for spatial heterogeneity in solar resources, transmission system access, and HDV charging station location.

We found that DERs were deployed across most HDV stations in the least-cost solution, indicating distributed energy solutions are economically competitive with centralized energy resources. DERs reduced total costs of refueling electric and hydrogen HDVs at a majority of charging stations by replacing 24% to 30% of their total electricity purchased from the grid with their on-site generation. Individual stations' cost savings

varied significantly based on their locations and load profiles. Among DER deployment, SMRs deployment made up more than 99% of deployed capacity while solar PV and battery storage deployments combined made up less than 1%. Overall, these results demonstrate that DERs, particularly SMRs, can be an integral part of a least-cost pathway for serving emerging HDV charging demand. SMR deployment was favored at stations with flatter load profiles and in higher hydrogen penetration scenarios.

We tested the robustness of our results through sensitivity analysis to uncertainty in SMR and transmission line capital costs, transmission line utilization capabilities, and future wholesale electricity prices. Unless SMR capital cost is extremely more expensive that current estimate (100% more expensive than reference case), we found that the market for SMRs would be large (at last 5.7 GW) across these sensitivities. Installed capacities and cost savings from SMR investments were most sensitive to future SMR capital costs and wholesale electricity prices. Specifically, lower SMR capital costs and higher and/or more volatile electricity prices would increase deployment of and cost savings from SMRs.

Our analysis adopts a station-centric perspective to meeting emerging HDV energy demands. However, emerging HDV energy demands will in the aggregate affect regional energy demand, and could in turn be met with regional energy solutions. We do not capture interactions between local DER investments, regional energy demand, and regional electricity prices, but instead assume regional prices do not vary with local DER investments. This interaction is likely minor, as future decarbonized HDV energy demands will be small relative to total regional demand. Nonetheless, future work could capture interactions between regional and local investments through a macro-energy system model, e.g. a capacity expansion model. The drawback of this approach is that these macro-scale models are so computationally intensive that they require significant simplifications in data inputs, which could elide important spatiotemporal heterogeneity across stations.

A macro-scale approach could also quantify the value of DERs in enabling system-wide greenhouse gas emission reductions.

This paper has several other limitations that future work can address. First, our analysis assumed HDV charging stations would purchase electricity at the wholesale rather than retail rate. Since retail rates exceed wholesale prices, stations purchasing electricity at retail rates would likely see more value from DER deployment. Similarly, the mid-case price scenario we use does not account for the capacity expansion required in a scenario where HDVs are fully electrified and therefore may underestimate prices. Second, to buy electricity from the grid, we assumed that charging stations have to build new transmission lines of voltage class high enough to serve their peak loads. In reality, given the physical difficulties, regulatory obstacles, and social opposition of constructing new long distance high voltage transmission lines, charging stations are more likely to explore upgrading existing transmission lines to higher voltage classes to minimize these challenges. However, routing along existing infrastructure would also present challenges as structures and right-of-ways would need to be upgraded/expanded for higher voltage lines. Third, our analysis assumed each station requires additional transmission capacity to buy bulk power and thus did not capture existing transmission capacity to stations below 69 kV. This assumption could lead to overestimation of transmission expansion costs. Finally, our model assumed a static transmission system that stays the same in all different electricity price times series scenarios (2030, 2040, and 2050). This assumption could also potentially result in overestimation of transmission expansion costs, e.g. if significant transmission expansion occurs for broader decarbonization purposes. However, as noted previously, significant uncertainty surrounds future transmission expansion due to regulatory, political, and social acceptability hurdles. Overall, though, we believe these limitations do not significantly impact the robustness of our results because transmission expansion cost not only makes up a small percentage of total cost of meeting HDV energy

demand (less than 10% in a 100% electric HDV fleet, and in the cases of higher levels of hydrogen HDV demand, 3%), but also has minimal impacts on stations' DER investment decisions as demonstrated by our sensitivity analyses.

5 Conclusion

Decarbonizing the HDV fleet via electricity and/or hydrogen is crucial to limit global warming below 1.5°C or 2°C above the pre-industrial levels. HDVs pose a bigger challenge in transitioning compared to smaller vehicles due to their sizes and weights, but little research has explored different avenues for meeting decarbonized HDV energy demand. In this paper, we use a technoeconomic optimization model with high spatiotemporal resolution to compare between distributed versus centralized energy sources for charging electric and/or refueling hydrogen HDVs. We apply this model to solar PV, battery, and SMR DER options at 167 charging stations across the United States. We find that for a wide ranges of scenarios, DERs - and specifically SMRs - can be viable resources for decarbonizing the HDV fleet. SMR value and deployment increases with increasing hydrogen HDVs, decreasing SMR capital costs, and increasing wholesale electricity prices. Investments in DERs can offer annual cost savings up to over $1.9 billion across all charging stations, with individual charging station's annual cost-saving up to over $104 million. These findings emphasize the potential market competitiveness of DERs to provide energy input for HDV energy demand and the large role that the emerging HDV energy market could play for the emerging SMR technology. Future research on meeting decarbonized HDV energy demands should extend our analysis by capturing retail electricity rates, upgrading existing transmission corridors, and integrating distributed energy options for charging stations within macro-scale power system models.

6 Acknowledgement

We thank Steven Aumeier and John Smart from the Idaho National Laboratory for their helpful suggestions and feedbacks. We also thank Fan Tong and Corinne D. Scown from Lawrence Berkeley National Laboratory, Alex Monn from Midcontinent Independent System Operator, Maxwell Brown from the National Renewable Energy Laboratory, Liza Reed of the Niskanen Center, and Maxwell Woody from University of Michigan for invaluable data guidance and suggestions. We also thank Yifan Luo from the University of Michigan for GIS assistance. Funding for this research was provided by the Idaho National Laboratory's Emerging Energy Markets Analysis initiative and the National Science Foundation Graduate Research Fellowship Program (for Larson Lovdal). We are grateful to both funding sources.

References

[1] IPCC, Global Warming of 1.5°C. An IPCC Special Report on the Impacts of Global Warming of 1.5°C above Pre-industrial Levels and Related Global Greenhouse Gas Emission Pathways, in the Context of Strengthening the Global Response to the Threat of Climate Change, Sustainable Development, and Efforts to Eradicate Poverty., Final Report., Intergovernmental Panel on Climate Change (2018).

[2] EIA, Monthly Energy Review., Tech. rep., U.S. Energy Information Administration (2017).

[3] EPA, Inventory of U.S. Greenhouse Gas Emissions and Sinks: 1990-2019., Final Report., US Environmental Protection Agency (2021).

[4] DOE, Vehicle Weight Classes & Categories (2011).

[5] IEA, The Future of Trucks, Tech. rep., International Energy Agency (2017).

[6] P. Kluschke, T. Gnann, P. Plötz, M. Wietschel, Market Diffusion of Alternative Fuels and Powertrains in Heavy-duty Vehicles: A Literature Review, Energy Reports 5 (2019) 1010–1024.

[7] G. Aydin, The Modeling and Projection of Primary Energy Consumption by the Sources, Energy Sources, Part B: Economics, Planning, and Policy 10 (1) (2015) 67–74.

[8] IEA, Net Zero by 2050: A Roadmap for the Global Energy Sector, Tech. rep., International Energy Agency (2021).

[9] DOE, U.S. Plug-in Electric Vehicle Sales by Model (2020).

[10] DDPP, Pathways to Deep Decarbonization., Tech. rep., Deep Decarbonization Pathways Project (2015).

[11] S. J. Davis, N. S. Lewis, M. Shaner, S. Aggarwal, D. Arent, I. L. Azevedo, S. M. Benson, T. Bradley, J. Brouwer, Y.-M. Chiang, C. T. M. Clack, A. Cohen, S. Doig, J. Edmonds, P. Fennell, C. B. Field, B. Hannegan, B.-M. Hodge, M. I. Hoffert, E. Ingersoll, P. Jaramillo, K. S. Lackner, K. J. Mach, M. Mastrandrea, J. Ogden, P. F. Peterson, D. L. Sanchez, D. Sperling, J. Stagner, J. E. Trancik, C.-J. Yang, K. Caldeira, Net-zero Emissions Energy Systems, Science 360 (6396) (2018).

[12] H. Fayaz, R. Saidur, N. Razali, F. Anuar, A. Saleman, M. Islam, An Overview of Hydrogen as a Vehicle Fuel, Renewable and Sustainable Energy Reviews 16 (8) (2012) 5511–5528.

[13] F. H. Sobrino, C. R. Monroy, J. L. H. Pérez, Critical Analysis on Hydrogen as an Alternative to Fossil Fuels and Biofuels for Vehicles in Europe, Renewable and Sustainable Energy Reviews 14 (2) (2010) 772–780.

[14] M. Granovskii, I. Dincer, M. A. Rosen, Economic and Environmental Comparison of Conventional, Hybrid, Electric and Hydrogen Fuel Cell Vehicles, Journal of Power Sources 159 (2) (2006) 1186–1193.

[15] W. Colella, M. Jacobson, D. Golden, Switching to a U.S. Hydrogen Fuel Cell Vehicle Fleet: The Resultant Change in Emissions, Energy Use, and Greenhouse Gases, Journal of Power Sources 150 (2005) 150–181.

[16] P. K. Rose, F. Neumann, Hydrogen Refueling Station Networks for Heavy-duty Vehicles in Future Power Systems, Transportation Research Part D: Transport and Environment 83 (2020) 102358.

[17] E. Çabukoglu, G. Georges, L. Küng, G. Pareschi, K. Boulouchos, Fuel Cell Electric Vehicles: An Option to Decarbonize Heavy-duty Transport? Results from a Swiss Case-study, Transportation Research Part D: Transport and Environment 70 (2019) 35–48.

[18] C. Murphy, T. Mai, Y. Sun, P. Jadun, P. Donohoo-Vallett, M. Muratori, R. Jones, B. Nelson, High Electrification Futures: Impacts to the U.S. Bulk Power System, The Electricity Journal 33 (10) (2020) 106878.

[19] F. Tong, A. Jenn, D. Wolfson, C. D. Scown, M. Auffhammer, Health and Climate Impacts from Long-Haul Truck Electrification, Environmental Science & Technology 55 (13) (2021) 8514–8523.

[20] S. P. Vajjhala, P. S. Fischbeck, Quantifying Siting Difficulty: A Case Study of U.S. Transmission Line Siting, Energy Policy 35 (1) (2007) 650–671.

[21] N. Cain, H. Nelson, What Drives Opposition to High-voltage Transmission Lines?, Land Use Policy 33 (2013) 204–213.

[22] A. Q. Gilbert, M. D. Bazilian, Can Distributed Nuclear Power Address Energy Resilience and Energy Poverty?, Joule 4 (9) (2020) 1839–1843.

[23] M. R. Abdussami, H. A. Gabbar, Nuclear-Powered Hybrid Energy Storage-Based Fast Charging Station for Electrification Transportation, 2019 IEEE 7th International Conference on Smart Energy Grid Engineering (SEGE) (2019) 304–308.

[24] J. Buongiorno, B. Carmichael, B. Dunkin, J. Parsons, D. Smit, Can Nuclear Batteries Be Economically Competitive in Large Markets?, Energies 14 (4385) (2021).

[25] M. G. Morgan, A. Abdulla, M. J. Ford, M. Rath, U.S. Nuclear Power: The Vanishing Low-carbon Wedge, Proceed to National Academy of Sciences 115 (28) (2018) 7184–7189.

[26] L. M. Boldon, P. Sabharwall, Small Modular Reactor: First-of-a-Kind (FOAK) and Nth-of-a-Kind (NOAK) Economic Analysis, Idaho National Lab (2014).

[27] B. Vegel, J. C. Quinn, Economic Evaluation of Small Modular Nuclear Reactors and the Complications of Regulatory Fee Structures, Energy Policy 104 (2017) 395–403.

[28] M. Ruth, P. Spitsen, R. Boardman, Opportunities and Challenges for Nuclear-Renewable Hybrid Energy Systems, Tech. rep., National Renewable Energy Laboratory (2019).

[29] D. T. Ingersoll, Z. J. Houghton, R. Bromm, C. Desportes, Integration of NuScale SMR With Desalination Technologies, ASME 2014 Small Modular Reactors Symposium, SMR 2014 ASME 2014 Small Modular Reactors Symposium (2014).

[30] McMillan, C. A., M. Ruth, Using Facility-level Emissions Data to Estimate the Technical Potential of Alternative Thermal Sources to Meet Industrial Heat Demand, Applied Energy 239 (2019).

[31] M. Nichol, H. Desai, Cost Competitiveness of Micro-Reactors for Remote Markets, Tech. rep., Nuclear Energy Institute (NEI) (2019).

[32] N. Edson, P. Willson, B. Rakshi, I. Kekwick, Market and Technical Assessment of Micro Nuclear Reactors, Tech. rep., Nuvia (2016).

[33] MISO, Transmission Cost Estimation Guide (2021).

[34] ESRI, ArcGIS Pro (Version 2.8) (2021).

[35] DHS, Homeland Infrastructure Foundation-Level Data (2021).

[36] USDA, National Agricultural Statistics Service (2017).

[37] J. Dewitz, National Land Cover Database (NLCD) 2019 v2 (2021).

[38] BPA, 2010 Electric Transmission & Distribution Benchmarking (2011).

[39] ATB, Electricity Annual Technology Baseline (2020).

[40] FEMP, 2021 Discount Rates, official memorandum, Department of Energy, Washington, DC, USA (2021.).

[41] I. Bromley-Dulfano, J. Florez, M. T. Craig, Reliability Benefits of Wide-area Renewable Energy Planning across the Western United States, Renewable Energy 179 (2021) 1487–1499.

[42] NREL, Cambium Dataset (2020).

[43] G. A. Black, F. Aydogan, C. L.Koerner, Economic Viability of Light Water Small Modular Nuclear Reactors: General Methodology and Vendor Data, Renewable and Sustainable Energy Reviews 103 (2019) 248–258.

[44] J. A. Dowling, K. Z. Rinaldi, T. H. Ruggles, S. J. Davis, M. Yuan, F. Tong, N. S. Lewis, K. Caldeira, Role of Long-Duration Energy Storage in Variable Renewable Electricity Systems, Joule 4 (9) (2020) 1907–1928.

[45] N. A. Sepulveda, J. D. Jenkins, A. Edington, D. S. Mallapragada, R. K. Lester, The Design Space for Long-duration Energy Storage in Decarbonized Power Systems, Nature Energy 6 (2021) 506–5016.

[46] NREL, H2A: Hydrogen Analysis Production Models, Tech. rep., National Renewable Energy Laboratory (2018).

[47] W. Cole, S. Corcoran, N. Gates, T. Mai, P. Das, 2020 Standard Scenarios Report: A U.S. Electricity Sector Outlook, Tech. rep., National Renewable Energy Laboratory (2020).

[48] P. Gagnon, W. Frazier, E. Hale, W. Cole, Cambium Documentation: Version 2020, Tech. rep., National Renewable Energy Laboratory (2020).

[49] TE, Comparison of Hydrogen and Battery Electric Trucks - Methodology and Underlying Assumptions, Tech. rep., European Federation for Transport and Environment (2020).

[50] E. G. Giakoumis, G. Triantafillou, Analysis of the Effect of Vehicle, Driving and Road Parameters on the Transient Performance and Emissions of a Turbocharged Truck, Energies 11 (2) (2018).

[51] S. Sripad, V. Viswanathan, Performance Metrics Required of Next-Generation Batteries to Make a Practical Electric Semi Truck, ACS Energy Letters 2 (7) (2017) 1669–1673.

[52] Y.-Q. Zhao, H.-Q. Li, F. Lin, J. Wang, X.-W. Ji, Estimation of Road Friction Coefficient in Different Road Conditions Based on Vehicle Braking Dynamics, Chinese Journal of Mechanical Engineering 30 (2017) 982–990.

[53] S. Ramachandran, U. Stimming, Well to Wheel Analysis of Low Carbon Alternatives for Road Traffic, Energy Environ. Sci. 8 (2015) 3313–3324.

[54] D. Smith, R. Graves, B. Ozpineci, P. T. Jones, J. Lustbader, K. Kelly, K. Walkowicz, A. Birky, G. Payne, C. Sigler, J. Mosbacher, Medium- and Heavy-Duty Vehicle Electrification: An Assessment of Technology and Knowledge Gaps, Tech. rep., Office of Energy Efficiency and Renewable energy, U.S. Department of Energy (2019).

[55] C. Cunanan, M.-K. Tran, Y. Lee, S. Kwok, V. Leung, M. Fowler, A Review of Heavy-Duty Vehicle Powertrain Technologies: Diesel Engine Vehicles, Battery Electric Vehicles, and Hydrogen Fuel Cell Electric Vehicles, Clean Technologies 3 (2) (2021) 474–489.

[56] C. Iclodean, B. Varga, N. Burnete, D. Cimerdean, B. Jurchiș, Comparison of Different Battery Types for Electric Vehicles, IOP Conf. Series: Materials Science and Engineering 252 (2017).

[57] J. Marcinkoski, R. Vijayagopal, J. Kast, A. Duran, Driving an Industry: Medium and Heavy Duty Fuel Cell Electric Truck Component Sizing, World Electric Vehicle Journal 8 (1) (2016) 78–89.

[58] Z. Yu, D. Zinger, A. Bose, An Innovative Optimal Power Allocation Strategy for Fuel Cell, Battery and Supercapacitor Hybrid Electric Vehicle, Journal of Power Sources 196 (4) (2011) 2351–2359.

[59] ESRI, USA Counties (Generalized) (2021).

Supplementary Material

A Techno-economic Analysis of Distributed Energy Resources versus Wholesale Electricity Purchases for Fueling Decarbonized Heavy Duty Vehicles

For Online Publication.

Appendix A Model Overview

The HDV Charging Model is an optimization-based techno-economic model that minimizes total annual costs of meeting HDV energy demand at the charging station level, subject to technology and power system constraints.. Annual total costs equal the sum of capital costs in transmission and DERs; operational costs of transmission infrastructure and distributed energy capacity resources; and wholesale electricity purchase costs.

Appendix B Functional Forms

Appendix B.1 Battery Storage Capacity Expansion and Operating Costs

The annual total cost to expand k_s^B MW of new battery power rating, e_s^B MWh of battery energy capacity, and produce g_{st}^B MWh of battery storage generation at charging station s for all hour t in a given year is given by:

$$TC_s^B = p^{BK} k_s^B + p^{BC} e_s^B + \sum_t p^{BE} g_{st}^B, \tag{B.1}$$

where p^{BK} is the annualized battery power rating cost in \$/MW-year, p^{BC} is the battery energy capacity cost in \$/MWh, and p^{BE} is the battery operating cost in \$/MWh.

In addition, hourly battery inflow and generation at charging station s, d_{st}^B and g_{st}^B

respectively, are limited to the battery's power rating:

$$0 \leq d^B_{st} \leq k^B_s, \quad \forall s \in \mathbb{S}, \forall t \in \mathbb{T} \tag{B.2a}$$

$$0 \leq g^B_{st} \leq k^B_s, \quad \forall s \in \mathbb{S}, \forall t \in \mathbb{T} \tag{B.2b}$$

where k^B_s is battery's power rating at charging station s, $\mathbb{S}$ is the set of charging stations, and $\mathbb{T}$ is is the set of hours.

Battery generation at charging station s at time t is also limited to the battery's state of charge at that particular hour, x^B_{st}, which cannot exceed battery's energy capacity e^B_s:

$$0 \leq g^B_{st} \leq x^B_{st} \leq e^B_s, \quad \forall s \in \mathbb{S}, \forall t \in \mathbb{T} \tag{B.3}$$

Battery energy capacity depends on our assumption of battery hours h^B:

$$e^B_s = h^B k^B_s, \quad \forall s \in \mathbb{S} \tag{B.4}$$

Finally, the state of charge of battery at station s at time t also has to equal to the state of charge in previous hour, $t-1$ plus the battery inflow in current hour, and minus generation in current hour:

$$x^B_{st} = x^B_{s(t-1)} + d^B_{st} - g^B_{st}, \quad \forall s \in \mathbb{S}, \forall t \in \mathbb{T} \tag{B.5}$$

where $x^B_{s(t-1)}$ is the state of charge of battery at charging station s and at time $t-1$. The initial battery state of charge is assumed to equal to the state of charge in the last hour, $t = 8760$, plus the battery inflow and minus generation in the first hour:

$$x^B_{s(t=1)} = x^B_{s(t=8760)} + d^B_{t=1)} - g^B_{s(t=1)}, \quad \forall s \in \mathbb{S}, \forall t \in \mathbb{T} \tag{B.6}$$

Appendix B.2 Hydrogen Storage Capacity Expansion and Operating Costs

The annual total cost to expand k_s^H MW of new hydrogen power rating, e_s^H kg of hydrogen energy capacity, and produce g_{st}^H kg of battery storage generation at charging station s for all hour t in a given year is given by:

$$TC_s^H = p^{HK} k_s^H + p^{HC} e_s^H + \sum_t p^{HE} g_{st}^H, \tag{B.7}$$

where p^{HK} is the annualized hydrogen power rating cost in \$/MW-year, p^{HC} is the hydrogen energy capacity cost in \$/kg, and p^{HE} is the hydrogen operating cost in \$/kg.

In addition, hourly hydrogen inflow and generation at charging station s, d_{st}^H and g_{st}^H respectively, are limited to the its power rating:

$$0 \leq \left(\frac{1}{c^H}\right) d_{st}^H \leq k_s^H, \quad \forall s \in \mathbb{S}, \forall t \in \mathbb{T} \tag{B.8a}$$

$$0 \leq \left(\frac{1}{c^H}\right) g_{st}^H \leq k_s^H, \quad \forall s \in \mathbb{S}, \forall t \in \mathbb{T} \tag{B.8b}$$

where k_s^H is hydrogen's power rating at charging station s in MW and c_H is kg to MWh conversion.

Hydrogen generation at charging station s at time t is also limited to the its state of charge at that particular hour, x_{st}^H, which cannot exceed its energy capacity e_s^H:

$$0 \leq g_{st}^H \leq x_{st}^H \leq e_s^H, \quad \forall s \in \mathbb{S}, \forall t \in \mathbb{T} \tag{B.9}$$

The state of charge of hydrogen at station s at time t also has to equal to the state of charge in previous hour, $t-1$ plus the hydrogen inflow in current hour, and minus its

generation in current hour:

$$x^H_{st} = x^H_{s(t-1)} + d^H_{st} - g^H_{st}, \quad \forall s \in \mathbb{S}, \forall t \in \mathbb{T} \tag{B.10}$$

where $x^H_{s(t-1)}$ is the state of charge of hydrogen at charging station s and at time $t-1$. The initial hydrogen state of charge is assumed to be equal to the state of charge in the last hour, $t = 8760$, plus the hydrogen inflow and minus hydrogen generation in that first hour:

$$x^H_{s(t=1)} = x^H_{s(t=8760)} + d^H_{s(t=1)} - g^H_{s(t=1)}, \quad \forall s \in \mathbb{S}, \forall t \in \mathbb{T} \tag{B.11}$$

Appendix B.3 Solar Capacity Expansion and Operating Costs

The annual total cost to expand k^P_s MW of new solar power capacity, and produce g^P_{st} MWh of solar generation at charging station s for all hour t in a given year is given by:

$$TC^P_s = p^{PK}_s k^P_s + \sum_t p^{PE}_{st} g^P_{st}, \tag{B.12}$$

where p^{PK} is the annualized solar capital cost in \$/MW-year, and p^{PE} is the solar operating cost in \$/MWh.

Additionally, each solar PV system at charging station s has a limit on the amount of electricity it can produce at any given hour t, reflecting its available effective capacity:

$$0 \leq g^P_{st} \leq f^P_{st} k^P_s, \quad \forall s \in \mathbb{S}, \forall t \in \mathbb{T} \tag{B.13}$$

where k^P_s is solar capacity at charging station s, and f^P_{st} is the solar capacity factor at charging station s at time t, which will be discussed in details in below section.

Appendix B.4 SMR Capacity Expansion and Operating Costs

The annual total cost to expand u_s^M SMR modules, and produce g_{st}^M MWh of SMR generation at charging station s for all hour t in a given year is given by:

$$TC_s^M = p^{MK} u_s^M k^M + \sum_t p_{st}^{ME} g_{st}^M, \tag{B.14}$$

where p^{MK} is the annualized SMR capital cost in \$/MW-year, and p^{ME} is the SMR operating cost in \$/MWh, and u_s^M is the (whole) number of SMR modules built at charging station s.

The amount of electricity the SMR at charging station s can produce at any given hour t is limited to its capacity:

$$0 \leq g_{st}^M \leq u_s^M \bar{k}^M, \quad \forall s \in \mathbb{S}, \forall t \in \mathbb{T} \tag{B.15}$$

where $\bar{k}^M$ is the capacity of one SMR module.

The SMR system at any charging station s also need to follow its ramping constraint, which is assumed to be a percentage r_s^M of its total capacity:

$$g_{st}^M - g_{s(t-1)}^M \leq r_s^M u_s^M \bar{k}^M \tag{B.16a}$$

$$g_{s(t-1)}^M - g_{st}^M \leq r_s^M u_s^M \bar{k}^M, \tag{B.16b}$$

Finally, the SMR generation at charging station s at time t must be at least equal to a minimum stable load g_{min}^M:

$$g_{st}^M \geq u_s^M g_{min}^M, \quad \forall s \in \mathbb{S}, \forall t \in \mathbb{T} \tag{B.17}$$

Appendix B.5 Transmission Expansion and Wholesale Power Costs

The annual total cost of purchasing electricity from wholesale electricity markets equals the sum of annualized capital cost of expanding $\bar{k}_{si}^{W}$ MW of effective transmission capacity of class i at charging station s the cost of purchasing g_{st}^{W} MWh of electricity generation from the wholesale electricity markets to charging station s across all time periods t in a given year is given by:

$$TC_{s}^{W} = \sum_{i} \left(1 + p^{WO}\right) p_{si}^{WK} \bar{k}_{i}^{W} u_{si}^{W} + \sum_{t} p_{st}^{WE} g_{st}^{W}, \tag{B.18}$$

where p_{si}^{WK} is the annualized transmission capital cost in \$/MW-year for station s of capacity class i, $u_{si}^{W} \in \{0, 1\}$ is the binary decision variable that determines whether or not a transmission line of effective capacity $\bar{k}_{si}^{W}$ at charging station s is built, p_{st}^{WE} is the wholesale electricity price at charging station s at time t, and p^{WO} is overhead cost in percentage. Additionally, there can only be at most one transmission line of one capacity class being built at any station, therefore:

$$\sum_{i} u_{si}^{W} < 1. \tag{B.19}$$

Total transmission capital expense for a given station and voltage class is the sum of estimated transmission line capital - covering structures, conductors, land acquisition, site preparation, and soft costs - as well as substation costs. Capital costs are annualized using a capital recovery factor and annual operating and maintenance expenses are added to produce the final cost estimate. The methodology and costs are primarily derived from the [33] Transmission Cost Estimation Guide and are detailed in Appendix C.5.

Appendix B.6 Objective Function

The model's objective function is the sum of total annualized cost of expanding capacity and operation of battery storage, hydrogen storage, solar PV, SMR, transmission, and purchase of electricity from the wholesale electricity markets:

$$
\begin{aligned}
TC_s &= TC_s^B + TC_s^H + TC_s^P + TC_s^M + TC_s^W \\
TC_s &= \left[p^{BK} k_s^B + p^{BC} e_s^B + \sum_t p^{BE} g_{st}^B \right] + \left[p^{HK} k_s^H + p^{HC} e_s^H + \sum_t p^{HE} g_{st}^H \right] \\
&+ \left[p^{PK} k_s^P + \sum_t p^{PE} g_{st}^P \right] + \left[p^{MK} u_s^M \bar{k}^M + \sum_t p^{ME} g_{st}^M \right] \\
&+ \left[\sum_i \left(1 + p^{WO}\right) p_{si}^{WK} \bar{k}_{si}^W u_{si}^W + \sum_t p_{st}^{WE} g_{st}^W \right]
\end{aligned} \tag{B.20}
$$

Appendix B.7 Market Clearing Conditions

The HDV model must satisfy the market clearing conditions for both hydrogen and electricity:

$$
g_{st}^B + g_{st}^P + g_{st}^M + g_{st}^W \geq d_{st}^E + d_{st}^B + \left(\frac{1}{c^H} \right) d_{st}^H, \, \forall s \in \mathbb{S}, \, \forall t \in \mathbb{T} \tag{B.21a}
$$

$$
g_{st}^H \geq \bar{d}_{st}^H, \, \forall s \in \mathbb{S}, \, \forall t \in \mathbb{T} \tag{B.21b}
$$

where d_{st}^E is total electricity demand in time t at charging station s (MWh), d_{st}^B is the battery inflow in time t at charging station s (MWh), d_{st}^H is hydrogen inflow in time t at charging station s (kg), $\bar{d}_{st}^H$ is the total hydrogen demand in time t at charging station s (kg), which is assumed to be equal to a percentage of total electricity demand at station s at time t converted to kg of hydrogen from MWh of electricity using conversion factor

c^H. Conversion details are discussed in section Appendix B.9.

Appendix B.8 Model Solutions

The model solutions at each charging station s are the new capacity investments of battery storage, hydrogen, solar PV, SMR, and effective transmission capacity of particular capacity class, as well as the hourly generations and inflows (in case of battery storage and hydrogen storage) of battery storage, hydrogen, solar PV, SMR, and hourly electricity purchased from the wholesale electricity markets. These solutions are resulted from solving the optimization model described above with objective function (B.20) subject to constraints (B.2a), (B.2b), (B.3), (B.4), (B.5), (B.6), (B.8a), (B.8b), (B.9), (4c), (B.11), (B.12), (B.15), (B.16a), (B.16b), (B.17), (B.19), (B.21a), and (B.21b).

Appendix B.9 Electricity to Hydrogen Demand Conversion

Two major steps are concerned here, which are conversion from electricity demand (in kWh) of Battery Electric Vehicle (BEV) to the electricity demand (in kWh) of Fuel Cell Electric Vehicle (FCEV), and conversion from electricity demand (in kWh) of FCEV to hydrogen demand (in kg) of FCEV. For the first step, bottom-up physics-based models are introduced as below.

$$E = \int P(t)\, dt \tag{B.22a}$$

$$E = \int \frac{F_{drag} + F_{friction}}{\eta_1 \times \eta_2} \times v(t)\, dt \tag{B.22b}$$

$$F_{drag} = \frac{1}{2} \times \rho \times C_d \times A \times v^2 \tag{B.22c}$$

$$F_{friction} = \mu \times m \times g \tag{B.22d}$$

where E is energy, P(t) is power, F_{drag} is drag force, $F_{friction}$ is friction force, v(t) is velocity of the vehicle (which we assume a constant of 70mph), η_1 is drivetrain efficiency,

η_2 is battery efficiency for BEV and fuel cell efficiency for FCEV, ρ is density of air, C_d is coefficient of drag, A is frontal area, μ is coefficient of friction, m is mass of the vehicle, and g is the gravitational constant.

The only differences that lie between BEV and FCEV are battery/fuel cell efficiency and masses. For BEV, its mass consists of base, powertrain, payload and BEV battery. And for FCEV, its mass consists of base, powertrain, payload, FCEV battery, fuel cell and tank. The parameters of both vehicles are as below.

Parameter	BEV	FCEV	Source
ρ	1.2	1.2	–
g(N/kg)	9.81	9.81	–
A(m^2)	[4.65,7.2]	[4.65,7.2]	[50], [51]
C_d	[0.45,0.7]	[0.45,0.7]	[51]
μ	[0.2,0.8]	[0.2,0.8]	[52]
$m_{payload}$ (kg)	[12000,36000]	[12000,36000]	[51]
$m_{payload}$ + $m_{powertrain}$(kg)	[6000,8000]	[6000,8000]	[51]
η_1	[0.9,0.95]	[0.9,0.95]	[51], [53]
η_2	[0.9,0.96]	[0.45,0.55]	[53], [54], [55]
$m_{battery}$(kg)	[170,550]	[65,85]	[56], [57]
$m_{fuelcell}$(kg)	–	[125,220]	[57], [58]
m_{tank}(kg)	–	[270,340]	[57]

Table A.1: BEV and FCEV Parameters

Monte Carlo simulations are done on the random variables, and the average energy consumption ratio of FCEV to BEV is 1.857, with 25th percentile of 1.743 and 75th percentile of 1.962.

For the second step, we divide by the higher heating value (HHV) for hydrogen 39.4kWh/kg, which is defined as the amount of energy released by combusting a fuel from 25°C to 150°C considering latent heat of vaporization. The result is the energy demand ratio of FCEV (in kg) to BEV (in kWh) of 0.0471 kg/kWh. From these values, hy-

drogen demand and the corresponding electricity demand are calculated at each station as:

$$\bar{d}^H_{st} = Scenario\ \%\ H_2 \times d^E_{0,st} \times 0.0471 kWh/kg \tag{B.23}$$

$$d^E_{st} = (1 - Scenario\ \%\ H_2) \times d^E_{0,st} + \bar{d}^H_{st} \times 51.4 kWh/kg \tag{B.24}$$

where $\bar{d}^H$ is the hydrogen demand in kg at station s at time t, $d^E_{0,st}$ is the original electric HDV demand at station s and time t from [19] in kWh, d^E_{st} is the total station electricity demand under a given hydrogen scenario in kWh, the electricity to hydrogen electrolyzer rate of 51.4 kWh/kg is from [46], and round trip efficiency is captured as a constraint.

Appendix C Data

In this section, we discuss the data and intermediate steps to calculate the parameters that are used in the model.

Appendix C.1 Battery Storage Capital and Operating Costs

To determine the annualized battery storage capital cost p^{BK}, we obtain interest rate, r^B, fixed O&M cost, p^{BF}, and battery capital expenditure, $CAPEX^B$ from U.S. National Renewable Energy Laboratory (NREL)'s 2020 Electricity Annual Technology Baseline [39]. The annualized battery storage capital cost is calculated as:

$$p^{BK} = CAPEX^B \times CRF^B + p^{PF} \tag{C.1}$$

where $CRF^B = \dfrac{r^B}{1-(1+r^B)^{CRP^B}}$ is the capacity recovery factor (CRF) for battery storage, CRF^B is capacity recovery period, or life time of battery storage. $CAPEX^B$ is assumed to be moderate and for a 4-hour battery. All of these parameters are detailed in Table A.2.

Parameter	Unit	Data	Source
CAPEX	$/kW	$1,455.00	[39]
Capacity recovery period	years	15	[39]
Fixed OM cost	$/MW-year	$36.37	[39]
Fixed energy cost	$/kWh/h	$0.00	[39]
Operating cost	$/kWh	$0.00	[39]
Battery hour	hours	4	[39]
Round trip efficiency	–	0.85	[39]
Interest rate	–	0.15	[39]

Table A.2: Details of Battery Storage Parameters

Appendix C.2 Hydrogen Storage Capital and Operating Costs

Data to calculate hydrogen storage capital and operating costs are taken from [44] and [45] as detailed in Table A.3.

Parameter	Unit	Data	Source
BEV's to FCEV's energy demand ratio	kg/kWh	0.0471	Imputed (see Appendix B.9)
Electricity to hydrogen via electrolyzer	kWh/kg	51.4	[46]
Annualized capital cost	$/kW/h	0.0148	[44]
Fixed energy cost	$/kg	$39.4	[45]
Operating cost	$/kg	$0.00	[44]
Round trip efficiency	–	0.49	[44]

Table A.3: Details of Hydrogen Storage Parameters

Appendix C.3 Solar Capital and Operating Costs

Appendix C.3.1. Annualized Solar Capital Cost

To determine the annualized solar capital cost p^{PK}, we obtain solar capacity recovery period, CRP^P, interest rate, r^P, fixed O&M cost, and capital expenditure, $CAPEX^P$, for utility PV from [39]. The annualized solar capital cost is calculated as:

$$p^{PK} = CAPEX^P \times CRF^P + p^{PF} \tag{C.2}$$

where $CRF^P = \frac{r^P}{1-(1+r^P)^{CRP^P}}$ is the solar capacity recovery factor, and CRP^P solar capacity recovery period for solar PV. $CAPEX^P$ is assumed to be moderate. All of these parameters are detailed in Table A.4.

Appendix C.3.2. Solar Capacity Factors

Solar capacity factors are allowed to vary by hour and location of each charging station and are calculated by [41] using solar resource data from NREL's National Solar Radiation Data Base (NSRDB) in 2014. Hourly solar capacity factors in UTC time are downloaded based on the coordinates of our model's population of charging stations and then converted into station's location's local time.

Parameter	Unit	Data	Source
CAPEX	$/kW	$1,354	[39]
Capacity recovery period	years	30	[39]
Fixed OM cost	$/kW-year	$19	[39]
Operating cost	$/kWh	$0.00	[39]
Interest rate	–	0.15	[39]

Table A.4: Details of Solar PV Parameters

Appendix C.4 SMR Capital and Operating Costs

	Unit	Data	Source
SMR:			
CAPEX	$/kW	$2,616.00	[43]
Life time	years	40	[43]
Fixed OM cost	$/kW-year	$25.00	[43]
Variable OM cost	$/MWh	$0.75	[43]
Fuel cost	$/MWh	$8.71	[43]
Minimum stable load	% of capacity	0.5	[43]
Ramp rate	% of capacity	0.4	[43]
Module capacity	MW	60	[43]
Microreactor:			
CAPEX	$/kW	$3,000.00	[24]
Life time	years	20	[24]
Fixed OM cost	$/kW-year	$50.00	[24]
Variable OM cost	$/MWh	$0.00	[24]
Fuel cost	$/MWh	$8.71	[24]
Minimum stable load	% of capacity	0.5	[24]
Ramp rate	% of capacity	0.4	[24]
Module capacity	MW	10	[24]

Table A.5: Details of SMR and Microreactor Parameters

Appendix C.5 Transmission Expansion Costs and Wholesale Electricity Prices

Conductor Cost

Conductor costs include conductor, Optical Groundwire (OPGW), shield wire, and corresponding installation costs for each circuit. The assumed conductor characteristics for each transmission class are shown in Table A.6. The required conductor length includes 4% addition to the length described in Appendix C.5 to account for sag and waste [33]. For conductor costs, double circuits estimates are twice the single circuit cost.

	69kV	161kV	230kV	345kV	500kV
Size (kcmil)	477	795	795	795	954
Type	ACSS ('Flicker')	ACSS ('Cuckoo')	ACSS ('Cuckoo')	ACSS ('Cuckoo')	ACSR ('Cardinal')
Conductors per Circuit	1	1	1	2	3
Amp Rating[1](A)	1180	1650	1650	1650	996
Power Rating (MVA)	140	460	657	1972	2598
Cost per Mile	$53,465	$61,723	$61,723	$83,234	$113,742
Resistance[1] (Ω/mile)	0.227	0.137	0.137	0.137	0.12

Table A.6: Conductor Characteristics & Costs

Structure Cost

Structure costs account for material and installation costs for tangent, angle and dead end support structures. This analysis uses the steel tower costs and assumptions from [33] to estimate structure costs for each transmission class. The number of structures and associated cost per mile is listed in A.7 and A.8.

	69kV	161kV	230kV	345kV	500kV
Tangent (#/mile)	9	7	5	4.5	3
Running Angle (#/mile)	1	1	1	1	1
Non-angled Dead End (#/mile)	0.25	0.25	0.25	0.25	0.25
Angled Dead End (#/mile)	0.25	0.25	0.25	0.25	0.25
Cost per Mile	$528,430	$520,772	$580,308	$969,786	$1,104,267

Table A.7: Single Circuit Structure Assumptions & Costs

[1]Conductor characteristics from Southwire product documentation
ACSS: https://overheadtransmission.southwire.com/wp-content/uploads/2017/06/acss.pdf
ACSR: https://overheadtransmission.southwire.com/wp-content/uploads/2017/06/acsr.pdf

	69kV Double	161kV Double	230kV Double	345kV Double	500kV Double
Tangent (#/mile)	9.5	7.5	7	6	5
Running Angle (#/mile)	1	1	1	1	1
Non-angled Dead End (#/mile)	0.25	0.25	0.25	0.25	0.25
Angled Dead End (#/mile)	0.25	0.25	0.25	0.25	0.25
Cost per Mile	$849,838	$1,005,009	$1,150,818	$1,991,936	$2,254,661

Table A.8: Double Circuit Structure Assumptions & Costs

Land Costs

To calculate land costs associated with the modeled transmission lines, we define the route for each capacity class as the straight line distance from a given station to the nearest transmission line of sufficient capacity. Using ArcGIS Pro Version 2.8 [34], and right-of-way widths from MISO [33], we calculate the length, area in each county, and area of each land cover type along a line path.

We estimate the cost to obtain a new right-of-way for each line by combining the area per county data with the latest National Agricultural Statistics Service (NASS) county-level cropland values [36], assuming transmission lines will be built through open space of similar or lesser value. For cropland value, we use the 2017 NASS total agricultural land asset value, including buildings. For the few geographic areas not included in the NASS data (predominately independent cities in Virginia), we assign the value from the surrounding or majority adjoining county. As these areas are small and only 41 exist in the US, this assumption has minimal impact on any single transmission line. Finally, per [33] we include an additional $15,235 per acre for permitting and acquisition costs.

To estimate ROW preparation costs, we aggregate the 2019 National Land Cover Database (NLCD) [37] cover classifications to align with the terrain types in [33] as shown in A.9. Multiplying the total acreage per terrain type by the preparation cost per acre yields the ROW preparation estimate.

MISO Terrain Type	NLCD Cover Class(es)	MISO Preparation Cost ($/Acre)
Light Vegetation	21, 22, 23, 24, 31, 51, 52, 71, 72, 73, 74, 81, 82	272
Forest	41, 42, 43	5,176
Wetland	11, 90, 95	108,871
Mountain	12	6,729

Table A.9: Land Cover Types and Preparation Costs

For county data, we use the Esri authoritative U.S. counties data layer [59]. The specific ArcGIS workflow is:

1. Use the tool "Select Layer by Attribute" from "Data Management Toolset" to separately group all transmission lines into six classes according to their voltage class (below 100kV, 100-161kV, 220-287kV, 345kV, 500kV, 735kV and above).
2. Use "Generate Near Table" from "Proximity Toolset" to calculate distances and other proximity information between 219 stations and their nearest transmission line for each class, and write results to a new stand-alone table.
3. Use the tool "XY to Line" to generate geodetic connection lines constructed based on the values in the start and end x- and y-coordinate fields from previous analysis.
4. Use "Intersect" to compute the geometric overlapping intersection of connection lines and the USA Counties or Land Cover type layer.
5. Use the "Add Join" tool to join intersected segments to entire connection lines, and calculate the percentage of each county and land cover type.

For any transmission paths with area not included in the U.S. counties layer (i.e. large bodies of water), we correct the transmission line capital cost (excluding substations) by the percentage of missing distance. For instance, if 10 percent of a line is missing, the line capital cost is divided by 0.9 before being added to substation costs. Twenty-nine lines across all stations and transmission classes (total 1314) have greater than a five percent correction. The model was run with and without the correction and the resulting

investment decisions did not change. Therefore, we include the correction as the best available approach to developing the most reasonable total cost estimates given the data limitations.

Overhead, Financing, and Contingency Costs

Overhead items shared among projects include Project Management (estimated as 5.5%), Administrative & General Overhead (estimated as 1.5%), allowance for funds used during construction (7.5%), and Engineering, environmental studies, and commissioning (3.0%). Combined, these items sum to a 17.5% overhead estimate that is applied to the total project estimate before contingency. In addition, the estimates follow [33] methodology in including a general 30% contingency applied to the total project estimate to address the considerable uncertainty of a simplified cost per mile estimation approach.

The capital expense for a transmission line at a given capacity class and station is annualized ($/MW-Year) using a capital recovery factor (CRF). We assume a conservative line lifetime (capital recovery period) of 30 years and test scenarios with interest rates at three and seven percent. Annualized costs also include operations and maintenance expenses of $7,300.75 per circuit mile annually in 2021 dollars based on an average from seventeen utilities [38]. Maintenance expenses are inflated from 2009 dollars to 2021 using the federal consumer price index.

Substation Cost

Substation costs are from [33] and include the construction of a new substation at each end of the proposed transmission line with appropriate transformers sized according to the power ratings listed in A.6. The substation costs at each charging station include transformers to step-down voltage to 69kV from the delivery line voltage, which is the lowest voltage class available in [33]. Substation costs also include operations and maintenance expenses of $1,543.65 per MVA annually in 2021 dollars based on an average

from 12 utilities [38]. Maintenance expenses are inflated from January 2009 to January 2021 dollars using the federal consumer price index.

Wholesale Electricity Prices

Wholesale electricity prices at which charging stations purchase energy from to serve charging demands are taken from NREL's Cambium dataset [42]. These electricity prices are assumed to be the projected hourly marginal energy prices for year 2040 at the balancing authorities in which the charging stations are located. We choose to use 2040 data because this is the decade that is projected to start having rapid increase in renewable energy penetration to compensate for more rapid retirements of coal and nuclear plants [48].

Appendix D Model Code and Data Availability

Model code and data are available at https://github.com/atpham88/HDV.

All ArcGIS data (existing and modeled transmission lines, station locations, land cover layer) is available via an online map at https://umich.maps.arcgis.com/home/item.html?id=339298e71cb448ec8b4570c928b6f919.

Appendix E Lists of Model Variables, Parameters, Sets, and Full Model Formulation

Variable	Definition	Unit
k_s^B	Battery power rating at charging station s	MW
e_s^B	Energy capacity for battery at charging station s	MWh
g_{st}^B	Battery electricity discharge at charging station s at time t	MWh
d_{st}^B	Inflow demand for battery at charging station s at time t	MWh
x_{st}^B	State of charge for battery at charging station s at time t	MWh
k_s^H	H_2 power rating at charging station s	MW
e_s^H	Energy capacity for H_2 at charging station s	kg
g_{st}^H	H_2 discharge at charging station s at time t	kg
x_{st}^H	State of charge for H_2 at charging station s at time t	kg
d_{st}^H	Inflow demand for H_2 at charging station s at time t	kg
k_s^P	Solar capacity at charging station s	MW
g_{st}^P	Solar electricity generation at charging station s at time t	MWh
g_{st}^M	SMR electricity generation at charging station s at time t	MWh
u_s^M	Number of SMR modules to build at charging station s	Whole number
r^M	Ramping constraint for SMR at charging station s	%
u_{si}^W	Build (1) or not build (0) effective transmission capacity of class i at charging station s	Binary
g_{st}^W	Electricity purchased from wholesale markets to charging station s at time t	MWh

Table A.10: List of Variables

Parameter/Set	Definition	Unit
Parameters:		
p^{BK}	Battery annual capital cost	\$/MW-year
p^{BC}	Battery energy cost	\$/MWh
p^{BE}	Battery hours (= 4)	hour
p^{HK}	H_2 capital cost	\$/MW-year
p^{HC}	H_2 energy cost	\$/kg
p^{HE}	H_2 operating cost	\$/kg
$\bar{d}^{H}_{st}$	H_2 demand at charging station s at time t	kg
c^{H}	Conversion factor from 1 MWh to kg of H_2	–
p^{PK}	Solar capital cost	\$/MW-year
p^{PE}	Solar operating cost	\$/MWh
f^{P}_{st}	Solar capacity factor at charging station s at time t	%
g^{M}_{min}	SMR minimum stable load	MWh
p^{MK}	SMR capital cost	\$/MW-year
p^{ME}	SMR operating cost	\$/MWh
$\bar{k}^{M}$	SMR module capacity	MW
$\bar{k}^{W}_{si}$	Effective capacity transmission capacity of class i at charging station s	MW
p^{WK}_{si}	Annualized total cost of effective transmission capacity of class i at charging station s	\$/MW-year
p^{WE}_{st}	Wholesale electricity cost at charging station s at time t	\$/MWh
p^{WO}_{s}	Overhead add-ons at charging station s	%
d^{E}_{st}	Electricity demand at charging station s at time t	MWh
Sets:		
$\mathbb{I}$	Set of transmission capacity classes, index $i = \{1, 2, 3, ..., 5/10\}$	–
$\mathbb{S}$	Set of stations, index $s = \{1, 2, 3, ..., 170/161/152\}$	–
$\mathbb{T}$	Set of hours in a typical year, index $t = \{1, 2, 3, ..., 8760\}$	–
$\mathbb{Z}^{+}_{0}$	Set of whole numbers, $\mathbb{Z}^{+}_{0} = \{0, 1, 2, 3, ...\}$	–
$\mathbb{Z}_{2}$	Set of binary numbers, $\mathbb{Z}_{2} = \{0, 1\}$	–

Table A.11: List of Parameters and Sets

s.t.

General Non-negativity:	$k_s^B, k_s^H, k_s^P, k_s^W, e_s^B, e_s^H \geq 0,$	$\forall s \in \mathbb{S}$	(E.1)
Market Clearing Conditions:	$g_{st}^B + g_{st}^P + g_{st}^M + g_{st}^W \geq d_{st}^E + d_{st}^B + \left(\frac{1}{c^H}\right) d_{st}^H,$	$\forall s \in \mathbb{S}, \forall t \in \mathbb{T}$	(E.2)
Battery Constraints:	$0 \leq d_{st}^B \leq k_s^B,$	$\forall s \in \mathbb{S}, \forall t \in \mathbb{T}$	(E.3)
	$0 \leq g_{st}^B \leq k_s^B,$	$\forall s \in \mathbb{S}, \forall t \in \mathbb{T}$	(E.4)
	$0 \leq g_{st}^B \leq x_{st}^B,$	$\forall s \in \mathbb{S}, \forall t \in \mathbb{T}$	(E.5)
	$e_s^B = h^B k_s^B,$	$\forall s \in \mathbb{S}$	(E.6)
	$0 \leq x_{st}^B \leq e_s^B,$	$\forall s \in \mathbb{S}, \forall t \in \mathbb{T}$	(E.7)
	$x_{st}^B = x_{s(t-1)}^B + d_{st}^B - g_{st}^B,$	$\forall s \in \mathbb{S}, \forall t > 1 \in \mathbb{T}$	(E.8)
	$x_{s(t=1)}^B = x_{s(t=8760)}^B + d_{st}^B - g_{st}^B,$	$\forall s \in \mathbb{S}$	(E.9)
Hydrogen Constraints:	$0 \leq \left(\frac{1}{c^H}\right) d_{st}^H \leq k_s^H,$	$\forall s \in \mathbb{S}, \forall t \in \mathbb{T}$	(E.10)
	$0 \leq \left(\frac{1}{c^H}\right) g_{st}^H \leq k_s^H,$	$\forall s \in \mathbb{S}, \forall t \in \mathbb{T}$	(E.11)
	$0 \leq g_{st}^H \leq x_{st}^H,$	$\forall s \in \mathbb{S}, \forall t \in \mathbb{T}$	(E.12)
	$0 \leq x_{st}^H \leq e_s^H,$	$\forall s \in \mathbb{S}, \forall t \in \mathbb{T}$	(E.13)
	$x_{st}^H = x_{s(t-1)}^H + d_{st}^H - g_{st}^H,$	$\forall s \in \mathbb{S}, \forall t > 1 \in \mathbb{T}$	(E.14)
	$x_{s(t=1)}^H = x_{s(t=8760)}^H + d_{st}^H - g_{st}^H,$	$\forall s \in \mathbb{S}$	(E.15)
	$g_{st}^H \geq \bar{d}_{st}^H,$	$\forall s \in \mathbb{S}, \forall t \in \mathbb{T}$	(E.16)
Solar PV Constraints:	$0 \leq g_{st}^P \leq f_{st}^P k_s^P,$	$\forall s \in \mathbb{S}, \forall t \in \mathbb{T}$	(E.17)
SMR Constraints:	$0 \leq g_{st}^M \leq u_s^M \bar{k}^M,$	$\forall s \in \mathbb{S}, \forall t \in \mathbb{T}$	(E.18)
	$u_s^M \in \mathbb{Z}_0^+,$	$\forall s \in \mathbb{S}$	(E.19)
	$g_{st}^M \geq g_{min}^M,$	$\forall s \in \mathbb{S}, \forall t \in \mathbb{T}$	(E.20)
	$\|g_{st}^M - g_{s(t-1)}^M\| \leq r_s^M u_s^M \bar{k}^M,$	$\forall s \in \mathbb{S}, \forall t \in \mathbb{T}$	(E.21)
Wholesale Power Constraints:	$0 \leq g_{st}^W \leq \sum_i u_{si}^W \bar{k}_{si}^W,$	$\forall s \in \mathbb{S}, \forall t \in \mathbb{T}$	(E.22)
	$u_{si}^W \in \mathbb{Z}_2,$	$\forall s \in \mathbb{S}, \forall i \in \mathbb{I}$	(E.23)
	$\sum_i u_{si}^W \leq 1,$	$\forall s \in \mathbb{S}, \forall i \in \mathbb{I}$	(E.24)

Appendix F Additional Results

	Reference	SMR+10	SMR+20	SMR+30	SMR-10	SMR-20	SMR-30
Total Cost (Billion $)	8.62	8.75	8.85	8.94	8.48	8.33	8.17
SMR Deployment (GW)	9.54	8.16	6.90	5.70	10.38	10.60	12.60
No. DER Investing Stations	130	111	107	95	135	143	149

Table A.12: Sensitivity Analyses - Uncertainty in SMR Capital Costs

	Reference	Trans+30	Trans-30	Util 50	Util 30
Total Cost (Billion $)	8.62	8.88	8.34	8.83	9.19
SMR Deployment (GW)	9.54	9.60	9.54	10.9	11.70
No. DER Investing Stations	130	128	128	124	128

Table A.13: Sensitivity Analyses - Uncertainty in Transmission Costs and Transmission Line Utilization Factors

	Reference	LMP-2020	LMP-2030	LMP-2050
Total Cost (Billion $)	8.62	8.23	8.55	8.59
SMR Deployment (GW)	9.54	6.66	7.98	8.82
No. DER Investing Stations	130	104	112	127

Table A.14: Sensitivity Analyses - Uncertainty in Marginal Cost of Electricity

	100% Electric HDV Fleet	80% Electric+20% H_2 HDV Fleet	60% Electric+40% H_2 HDV Fleet
Total Cost (Billion $)	8.70	46.39	84.23
Cost Saving (Million $)	572 (6.2%)	684 (1.5%)	856 (1.0%)
From Power Purchase	2,516	2,996	3,456
From Infrastructure Upgrades	88	79	312
From Microreactor Generation	-512	-622	-768
From Microreactor Deployment	-1,000	-1,107	-1,355
From Battery and Solar Costs	-62	-26	-8
Microreactor Deployment (GW)	7.2	8.01	9.81
No. Microreactor Investing Stations	164 (98%)	166 (99%)	166 (99%)

Table A.15: Economic impacts of DER deployments (with microreactors).